E-Article

What Determines the Distinct Morphology of Species with a Particular Ecology? The Roles of Many-to-One Mapping and Trade-Offs in the Evolution of Frog Ecomorphology and Performance

Daniel S. Moen*

Department of Integrative Biology, Oklahoma State University, Stillwater, Oklahoma 74078

Submitted August 7, 2018; Accepted February 22, 2019; Electronically published August 26, 2019

Online enhancements: appendixes, supplemental material. *Dryad data:* https://doi.org/10.5061/dryad.n07742q.

abstract: Organisms inhabiting a specific environment often have distinct morphology, but the factors that affect this fit are unclear when multiple morphological traits affect performance in multiple behaviors. Does the realized morphology of a species reflect a compromise in performance among behaviors (i.e., trade-offs)? Or does many-to-one mapping result in morphological distinctness without compromising performance across behaviors? The importance of these principles in organismal design has rarely been compared at the macroevolutionary scale. Here I study 191 species of frogs from around the world that inhabit different microhabitats, using models of phenotypic evolution to examine how form-function relationships may explain the fit between ecology and morphology. I found three key results. First, despite being distinct in leg morphology, ecomorphs were similar in jumping performance. Second, ecomorphs that regularly swim showed higher swimming performance, which paralleled the higher leg muscle mass in these taxa. Third, many-to-one mapping of form onto function occurred at all but the highest levels of both jumping and swimming performance. The seemingly contradictory first two results were explained by the third: when one behavior occurs in all species while another is restricted to a subset, many-to-one mapping allows species with distinct ecologies to have distinct body forms that reflect their specialized behavior while maintaining similar performance in a more general shared behavior.

Keywords: anura, biomechanics, jumping, Ornstein-Uhlenbeck model, swimming.

Introduction

The study of ecomorphology has shown remarkably consistent and often convergent relationships between morphology and ecology across the tree of life (Wainwright and Reilly 1994; Losos 2011), for example, in plants (e.g., stem-succulent plants in deserts; Arakaki et al. 2011), fish (e.g., fish in general; East African cichlids in particular; Winemiller 1991; Muschick et al. 2012), and lizards (e.g., *Anolis*, Agamidae; Losos 1990; Melville et al. 2006). Such studies typically focus on the ways that ecomorphs are specialized for their particular ecology, yet often such distinct forms share aspects of ecology and behavior, making it unclear which ecologies and behaviors determine body form (Robinson and Wilson 1998). Moreover, many morphological characters have multiple functional roles (Endler 1995; Walker 2007; Bergmann and McElroy 2014), and finding how morphology differentially affects performance in those roles—or whether a difference even occurs—can be difficult.

Two themes of organismal design are often seen in nature when multiple concurrent functional demands are placed on organisms and those functions are determined by multiple morphological variables (Wainwright 2007; Bergmann and McElroy 2014). First, trade-offs in the effects of morphology on performance in multiple behaviors may affect the rate and direction of phenotypic evolution; selection may favor one body plan over another, depending on which behavior most affects fitness and how morphology affects performance in that behavior (Walker 2007; Holzman et al. 2011). In other words, the realized morphology of an ecomorph is expected to be the one that maximizes fitness (Parker and Maynard Smith 1990), even though that morphology would result in suboptimal performance for at least one other behavior (Alfaro et al. 2005).

Second, when several morphological variables affect a single function, multiple morphological configurations can produce the same functional value or performance (Wainwright et al. 2005; Marks and Lechowicz 2006; Wainwright 2007), alleviating potential trade-offs (Walker 2007; Holzman et al.

* Email: daniel.moen@okstate.edu.
ORCIDs: Moen, https://orcid.org/0000-0003-1120-0043.

Am. Nat. 2019. Vol. 194, pp. E81–E95.
DOI: 10.1086/704736

2011; Bergmann and McElroy 2014). This many-to-one mapping may free morphology to adapt to various selective demands without compromising current function (Alfaro et al. 2004, 2005; Wainwright 2007). The result is that while many different morphological forms could achieve equivalent performance in one function, the realized morphology of a species will likely be based on its other functions. This possibility has seldom been explored (Alfaro et al. 2005; Holzman et al. 2011), possibly because the many different functions of morphological traits are often unclear. Overall, trade-offs and many-to-one mapping are both potentially important for explaining the evolution of body form in many organisms because performance in many functions is frequently determined by multiple morphological variables (i.e., potential for many-to-one mapping) and many morphological variables influence multiple functions (i.e., potential for trade-offs; Endler 1995; Marks and Lechowicz 2006; Walker 2007). Thus, a key to disentangling these two principles is the study of how form relates to functional performance (Losos 1990; Wainwright and Reilly 1994; Koehl 1996; Losos 2011). Such studies can identify the consequences of differing morphology on performance and the ecological context of that performance.

Anuran amphibians (i.e., frogs and toads; "frogs" hereafter, for brevity) are an excellent group for examining the importance of many-to-one mapping and trade-offs in the evolution of ecomorphology. Most frog species can be categorized on the basis of microhabitat use (e.g., aquatic, arboreal, terrestrial; fig. 1; Moen and Wiens 2017), which is clearly reflected by their morphology (Moen et al. 2016; Citadini et al. 2018). Moreover, most ecomorphs occur around the world (Bossuyt and Milinkovitch 2000; Moen et al. 2013, 2016; Citadini et al. 2018), and convergent ecomorphs have evolved many independent times (fig. 1; Moen et al. 2016). This fit between ecology and morphology presumably relates to the different behaviors of species in these different microhabitats (e.g., climbing in arboreal frogs). However, many of these ecomorphs live in multiple environments (e.g., semiaquatic frogs regularly spend time both on land and in water), which means that in at least some cases the morphology of an ecomorph must affect performance in multiple different behaviors—some shared across ecomorphs (e.g., jumping; Gans and Parson 1966; Zug 1978; Marsh 1994; Shubin and Jenkins 1995) and others more specialized (e.g., swimming, climbing, burrowing, and walking; Emerson 1988; Reynaga et al. 2018). Importantly, each of these different behaviors may not favor the same morphological state. For example, while both long legs and muscular legs may increase jumping performance (Emerson 1978; Moen et al. 2013), swimming may favor increased muscle mass over leg length, as long legs would increase surface drag during the glide phase (Peters et al. 1996; Richards 2010). Yet the way that frogs swim and jump is at least superficially similar, as they generate thrust with powerful hindlimbs in both movements (Peters et al. 1996; Nauwelaerts et al. 2007; but see Gillis and Biewener 2000; Richards 2010). This means that it may be possible to simultaneously optimize performance in both behaviors with the same morphology (e.g., muscular legs). Alternatively, it may be advantageous for some types of frogs (e.g., climbing arboreal species) to have less muscular legs because muscle tissue is heavy, instead achieving high jumping performance through having longer legs. In sum, it remains unclear whether many-to-one mapping, trade-offs, both, or neither affects the importance of life in multiple environments in the evolution of the distinctive morphology of frog ecomorphs.

Here I test models of phenotypic evolution and relate body form to function to explain the distinctive leg morphology of different frog ecomorphs. I conducted extensive novel analyses on previously published data sets of microhabitat use, morphology, and performance from 191 species of frogs from 12 sites around the world. First, I modeled the dynamics of morphological evolution to test the distinctiveness of leg morphology across different microhabitats. Second, I used the same set of models to test whether high performance in jumping and swimming is equally vital across various microhabitats. Third, I estimated the evolutionary relationships between leg morphology and both jumping and swimming performance to explain contrasting results for morphology and performance in their relationship to microhabitat use. Overall, I show that many-to-one mapping alleviates potential trade-offs in the morphological variables that affect performance in multiple behaviors, allowing species to morphologically specialize in one behavior (e.g., swimming) without sacrificing high performance in another (e.g., jumping).

Material and Methods

Sampling and Data Collection

Moen et al. (2013) measured the locomotor performance and morphology of 44 species of anurans from Australia, China, and Colombia. They assigned species to four ecomorph categories based on adult activity and nonbreeding behavior: arboreal (living in trees), burrowing (digging their own burrows), semiaquatic (living at the interface of land and water), and terrestrial (spending nearly all adult life outside water). Subsequent work (Moen et al. 2016; Moen and Wiens 2017) added four additional categories, two of which pertain to the species examined here: aquatic (spending nearly all of their time in water) and torrential (living on vegetation and wet rocks in high-gradient streams). Based on these additional categories, I reclassified three species from Moen et al. (2013); see appendix A (apps. A, B are available online) for new classification and justification. To better characterize ecomorphs in terms of leg length and muscle mass, I also used the morphological data set of Moen et al. (2016), who examined museum specimens of 167 species collected at 10 sites around

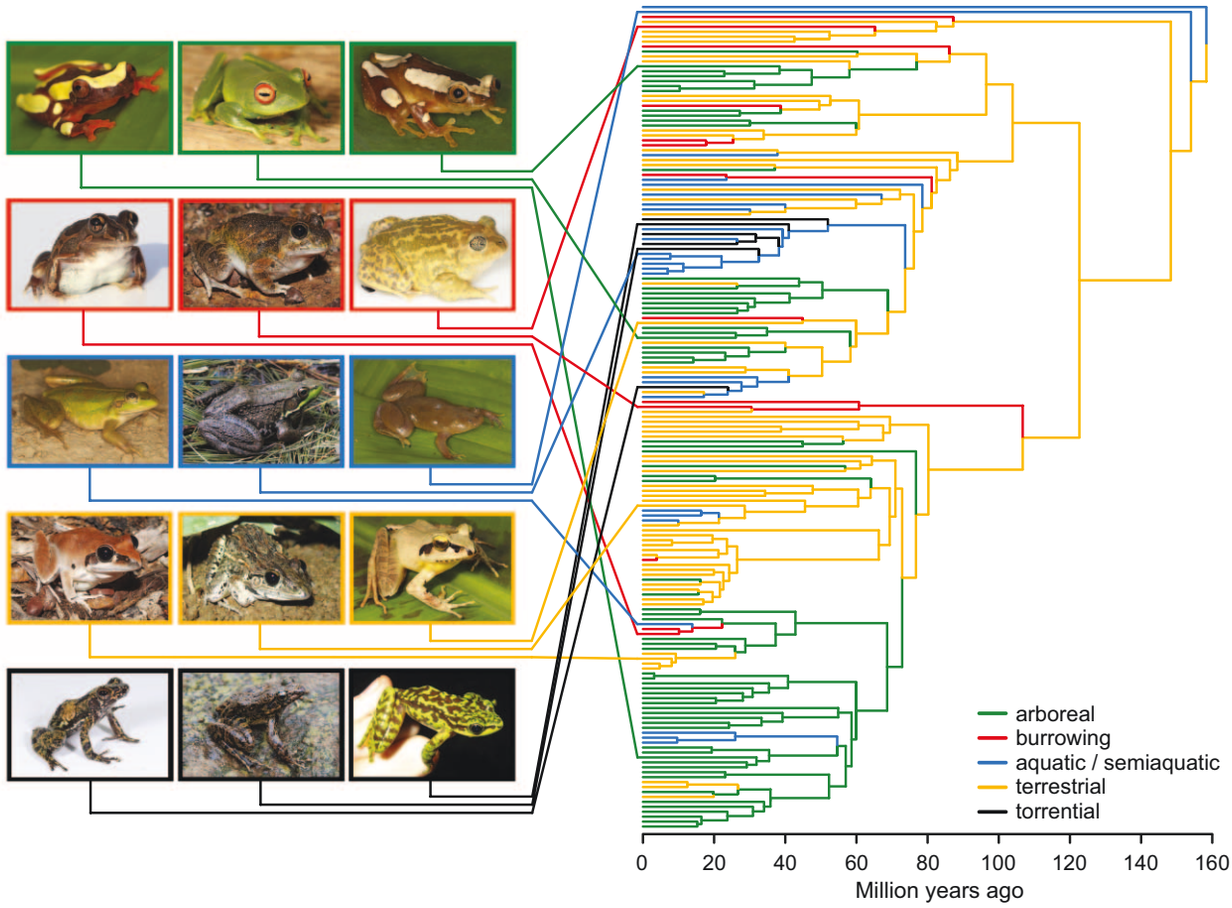

Figure 1: Evolution of ecomorphs in 167 species of anurans (Moen et al. 2016), spanning nearly their entire history (~160 myr). All types have repeatedly evolved in distantly related clades around the world. Aquatic and semiaquatic ecomorphs are shown in the same color as a visual aid. The phylogeny (*right*; modified from Moen et al. 2016) shows the maximum likelihood ancestral state estimates. Photos (*left*) show examples of the typical morphology for each ecomorph (*top to bottom*, *left to right*): arboreal (*Dendropsophus sarayacuensis*, *Boophis luteus*, *Afrixalus paradorsalis*); burrowing (*Cyclorana longipes*, *Platyplectrum ornatum*, *Spea bombifrons*); aquatic/semiaquatic (*Litoria dahlii*, *Rana clamitans*, *Xenopus tropicalis*); terrestrial (*Litoria tornieri*, *Leptodactylus fuscus*, *Aglyptodactylus madagascariensis*); and torrential (*Mantidactylus lugubris*, *Odorrana grahami*, *Amolops tuberodepressus*). The phylogenetic placement of some species used for photos is approximate, as they were not in the data set of Moen et al. (2016). The photo of *Odorrana* is used with permission from Jing Che; all other photos are by the author.

the world. Twenty species and one site were in both data sets, leading to a total here of 191 species across 12 sites. Appendix B lists all specimens used in the current study.

Moen et al. (2013) measured jumping, swimming, and clinging performance, analyzing data from those behaviors together as a composite performance phenotype in principal component space. In contrast, here I focus on only jumping and swimming performance and analyze them separately to link them directly to morphology. Detailed performance and morphological methods can be found in Moen et al. (2013, 2016). Briefly, jumping and swimming behavior were solicited (e.g., light tap on the animal's back) and recorded using a high-speed camera (Fastec TroubleShooter TS250MS). Trials were conducted at ambient temperatures (21.8°–27.6°C), a range over which previous studies of anuran jumping have shown similar performance (Wilson 2001; Navas et al. 2008; Careau et al. 2014). The snout was then digitized in each video frame, total displacement between frames was calculated from the *x*- and *y*-coordinates, and displacement-by-time curves were smoothed with a quintic spline (Walker 1998). Derivatives of these curves were used to estimate velocity and acceleration profiles, whose peak values defined each individual's maximum performance. Species means were estimated from these individual maxima and used for all analyses (see tables S2 and S3 of Moen et al. 2013). I study peak velocity and acceleration here because they are likely important in anuran ecology. For example, at a given takeoff angle (similar among these species; Moen et al. 2013), velocity largely

determines jumping distance (Marsh 1994), which can help frogs escape from predators (Emerson 1978; James et al. 2007). Additionally, acceleration might be directly favored by selection because it determines how quickly a frog may leap away (Emerson 1978; James et al. 2007). Note that while velocity and acceleration were calculated from the same initial data (i.e., displacement over time) and are correlated (see below), acceleration peaks earlier than velocity during movement (e.g., Gal and Blake 1988; Marsh and John-Alder 1994; James and Wilson 2008), decoupling the variables. Thus, they are distinct variables that both merit analysis.

After recording videos, frogs were euthanized and preserved to measure morphology. Here I focus on body length (snout-to-vent length [SVL]), body mass, leg length (from the posterior tip of the ischium to the tip of the foot), and total leg muscle mass. I examine these variables because all four affect jumping and swimming performance (e.g., Emerson 1978; Zug 1978; Marsh 1994; Choi and Park 1996; Choi et al. 2003; Nauwelaerts et al. 2007; Moen et al. 2013; Astley 2016; Citadini et al. 2018). Moen et al. (2016) collected data on the same variables from preserved museum specimens, and I combined their data set with that of Moen et al. (2013) for the 191-species morphological data set analyzed herein. All original data used for these analyses have been deposited in the Dryad Digital Repository (https://doi.org/10.5061/dryad.n07742q; Moen 2019).

Phylogeny

To analyze the morphology data set, I used the time-calibrated ultrametric phylogeny of Pyron (2014), pruning the 2,777-species anuran tree to include only the 191 species for which I had morphological data. Twenty of the 191 species were not in the phylogeny. Thus, I made similar substitutions as in previous studies (Moen et al. 2013, 2016), which should have little effect on my analyses (see the supplemental PDF for full list of substitutions and justification). For the performance analyses (44 species), I used the phylogeny from Moen et al. (2013), who used the topology of Pyron and Wiens (2011) and who calibrated branch lengths to time for that article (Moen et al. 2013). The topology of Pyron and Wiens (2011) was very similar to that of Pyron (2014), as the two trees are based on extensively overlapping molecular data sets. I provide the phylogenies used here in the supplemental PDF and in Dryad (https://doi.org/10.5061/dryad.n07742q; Moen 2019).

Statistical Analysis

Comparing Leg Morphology among Ecomorphs. To compare leg morphology among ecomorphs, I first calculated size-standardized (i.e., relative) leg length and muscle mass. I use relative (rather than absolute) variables because previous studies have shown that frog species with short legs for their body length have lower takeoff velocity than those with long relative leg length (RLL; Emerson 1978; Zug 1978; Choi et al. 2003; Gomes et al. 2009; Astley 2016). Likewise, given that muscles produce the force (and thus acceleration) necessary for moving a body's mass, higher relative leg muscle mass (RLMM) leads to higher velocity in jumping and swimming (Choi et al. 2003; Moen et al. 2013; Astley 2016). I calculated relative variables as ratios. Leg length was standardized by SVL and total leg muscle mass by total preserved body mass, given that muscle mass was measured from preserved muscles. In appendix A I justify using ratios over other approaches for analyzing relative variables, in particular showing that leg length and leg muscle mass scale isometrically with body length and body mass, respectively (table A1; fig. A1; tables A1–A8, table B1, and figs. A1–A7 are available online).

Second, I examined the relationship between RLL and RLMM by using a phylogenetic generalized least squares (PGLS) correlation (Martins and Hansen 1997). I calculated the correlation in R using equations from Rohlf (2006), correcting for the typical downward bias of product-moment correlations (Sokal and Rohlf 1995).

Finally, I compared models of phenotypic evolution to test whether ecomorphs are distinctive in RLL and RLMM. Previous studies have found that frog ecomorphs are similar in mean body size but distinctive in shape, with the latter based on an ordination of 10 morphological variables (Moen et al. 2013, 2016). However, those studies did not isolate the specific variables on which I focus here, so I explicitly tested them using Ornstein-Uhlenbeck (OU) models of adaptive evolution (Hansen 1997; Butler and King 2004). This test is necessary because if such variables did not differ across ecomorph types, form-function relationships between leg morphology and performance would not be able to explain ecomorphology.

For this test, I estimated and compared three models of evolution: Brownian motion (i.e., species similar only due to shared history), a single-optimum OU model (i.e., common morphology across ecomorphs), and a microhabitat-specific model that assigned a separate morphological optimum to each ecomorph (Moen et al. 2016; Scales and Butler 2016). Multistate OU models (as in the microhabitat model described above, with six different states) require specifying states for internal branches. I assigned internal states following previous anuran analyses (Moen et al. 2016), and these methods are described in detail in appendix A. Briefly, I used likelihood to compare models of discrete character evolution, estimated likelihood support for internal states under the optimal model, and assigned the state with the highest likelihood. I also considered other ways to assign internal states (including Bayesian stochastic character mapping, which accounts for uncertainty in internal state estimates; Huelsenbeck et al. 2003), but they gave nearly identical

results in the OU model fitting (app. A) and thus are not emphasized here. All internal state analyses were conducted with the R packages phytools (ver. 0.5-38; Revell 2012) and diversitree (ver. 0.9-9; FitzJohn 2012).

In these analyses I fit models for RLL and RLMM separately for simpler interpretation, but I also fit multivariate models that included both as response variables. While such multivariate model comparisons can be inaccurate with many traits (Adams and Collyer 2018), these problems do not occur with just two traits (app. A), multivariate methods can be more powerful for discriminating models (app. A), and these analyses only confirm the univariate tests (see "Results"). For these analyses and those that followed, I natural-log-transformed all morphological variables to fit statistical assumptions (linearity, normality, homogeneous variances) and biological expectations (many relationships among morphological variables are proportional or allometric; Pélabon et al. 2014). To compare models, I first calculated their likelihoods with ouch version 2.9-2 (Butler and King 2004; King and Butler 2009). I then used corrected Akaike information criterion (AICc) values and their weights to compare the relative statistical strength of each model (Burnham and Anderson 2002). Finally, I used parametric bootstrapping simulations (Boettiger et al. 2012) as an alternative way to compare models, to estimate the power of my model comparisons, and to calculate 95% confidence intervals for parameter estimates. In appendix A I give further justification for using OU models and detailed methods on parametric bootstrapping.

Comparing Jumping and Swimming Performance among Ecomorphs. As for leg morphology, I first used PGLS to examine the correlation between peak jumping and swimming velocity and acceleration to test whether performance in these two behaviors is conflicting (Nauwelaerts and Aerts 2003; Nauwelaerts et al. 2007), complementary (Gal and Blake 1987; Peters et al. 1996; Richards and Clemente 2013), or independent (Astley 2016). In particular, a trade-off between jumping and swimming performance would be indicated by a significant negative correlation between jumping and swimming velocity or acceleration.

Next, I tested whether different ecomorphs had distinct performance in jumping and swimming, an important (but untested) possibility that would speak to their distinct morphology. In other words, frogs are fundamentally jumping organisms (Gans and Parsons 1966; Zug 1978; Emerson 1979; Duellman and Trueb 1986; Lutz and Rome 1994; Marsh 1994), which suggests that most ecomorphs may be similar in jumping performance. Alternatively, some ecomorphs that are specialized for particular microhabitats (e.g., burrowing or aquatic) may have body forms that improve performance in their specialized behavior (e.g., burrowing or swimming) at the expense of high performance in jumping (Emerson 1976; Nauwelaerts et al. 2007).

For this comparison, I evaluated multiple models of performance evolution, focusing on OU models (Hansen 1997; Butler and King 2004) as described above. I emphasized separate analyses of velocity and acceleration but also conducted multivariate tests. For jumping performance, I compared the same three models as in morphology: Brownian motion, a single-optimum OU model, and an ecomorph-specific OU model. For swimming performance, I compared these same three models plus two more. The fourth model assigned one OU optimum to the three ecomorphs that regularly swim during nonbreeding adult life (aquatic, semiaquatic, and torrential) and a second optimum to those that do not (arboreal, burrowing, and terrestrial). The fifth model addressed breeding in water. Most species of frogs breed in water (Haddad and Prado 2005; Gomez-Mestre et al. 2012) and thus need to swim during reproduction, whether to reach calling sites, search for mates, or deposit eggs. For this model I used published breeding data (table A2) to assign taxa to either an optimum for water breeding or one for terrestrial breeding. Comparing these five models allowed me to test whether swimming performance is best modeled as similar across all species (single-optimum OU), idiosyncratic to ecomorph (microhabitat model), related to regular adult use of water (fourth model), or related to breeding in water (fifth model). I estimated and compared models as described above for morphology. Importantly, parametric bootstrapping simulations (as described above for morphology) showed that the low sampling of some ecomorph categories (e.g., two species of aquatic frogs) did not drastically reduce power to reject simpler models, at least for jumping and swimming velocity and multivariate analyses (app. A; figs. A6, A7). Finally, given that the swimming model was favored here (see "Results"), I revisited the jumping performance tests (by adding a swimming ecomorph model) to test whether the three swimming ecomorphs had both particularly high jumping and swimming performance, or just the latter.

Testing the Fit between Leg Morphology and Performance. I examined relationships between morphology and performance to understand how such relationships may affect the evolution of the distinctive morphology of ecomorphs. For this analysis I used PGLS regression (Martins and Hansen 1997), using the maximum likelihood value of λ (Pagel 1997; Freckleton et al. 2002; Revell 2010) to account for species similarity due to both common descent and shared predictor variables (Hansen and Orzack 2005). I examined the relationships between jumping and swimming peak velocity (response variables) and RLL, RLMM, total live frog mass, and ecomorph state (predictor variables). For brevity, I did not consider acceleration in these analyses given similar results in the OU model comparisons described above (see "Results"). I compared models of all possible combinations of the four predictor variables, totaling 15 candidate models for each

response variable. I used the R package caper (ver. 0.5.2; Orme et al. 2013) to estimate regression models, and I compared the different models using AICc values and their weights. Finally, I calculated standard partial regression coefficients of performance regressed on morphology to test for trade-offs (Walker 2007; Bergmann and McElroy 2014). Such coefficients would indicate trade-offs if a morphological variable had positive effects on one performance trait (e.g., jumping velocity) but negative effects on another (e.g., swimming velocity). See appendix A for a detailed explanation of this method.

Results

Comparing Leg Morphology among Ecomorphs

I found that ecomorphs differed significantly in leg morphology. Among the three evolutionary models of RLL evolution, the microhabitat-specific model was overwhelmingly favored (table 1). Likewise, the microhabitat-specific model was strongly favored for the evolution of RLMM (table 1). This same model was even more strongly favored for multivariate evolution of the two traits together (AICc weight = 1.0). Parametric bootstrapping simulations gave the same results (app. A). Examination of the OU optima (table A3) shows that RLL is similar across most ecomorphs, but burrowing species have particularly short legs for their body length, whereas torrential species have particularly long legs (fig. 2). Moreover, the three ecomorphs whose RLMM was higher are those that regularly swim in the nonbreeding season (aquatic, semiaquatic, and torrential; fig. 2).

RLL and RLMM are positively correlated across all ecomorphs ($r = 0.585$, df = 189, $P < .001$; fig. 3). This correlation was incorrectly reported as a negative correlation ($r = -0.53$) in a prior article (Moen et al. 2013); the latter was rather the negative correlation between parameter estimates of the effect of these variables on jumping velocity. In other words, a frog whose longer legs made it jump well tended to have smaller leg muscles, and a frog whose high jumping performance was caused by big leg muscles tended to have shorter legs (see below). Despite the strong positive correlation found here between morphological variables, considerable residual variation in RLMM occurs at a given RLL and vice versa. Generally, semiaquatic and aquatic species have relatively high leg muscle mass at a given RLL, whereas arboreal species often have relatively low leg muscle mass for their leg length (fig. 3). Burrowing, terrestrial, and torrential species are distributed roughly equally along the main axis of variation (fig. 3). To test these patterns statistically, I conducted an additional OU model comparison in which I standardized leg muscle mass by leg length (simply dividing leg muscle mass by leg length). This analysis showed that arboreal species have significantly low muscle mass for their leg length and that aquatic and semiaquatic species have high muscle mass, whereas the other three ecomorphs were intermediate (table A4).

Comparing Jumping and Swimming Performance among Ecomorphs

Peak jumping and swimming velocity were positively correlated across species ($r = 0.764$, df = 42, $P < .001$). Similarly, peak jumping and swimming acceleration were positively correlated, but more weakly ($r = 0.386$, df = 42, $P = .010$).

The optimal evolutionary model for jumping velocity was a single-peak OU model (table 2), indicating that regardless of ecomorph type, species have evolved toward similar jumping velocity over macroevolutionary time. Similarly, the single-peak OU model and Brownian motion showed similar statistical support for the evolution of jumping acceleration, with the latter slightly favored (table 2). Multivariate models of jumping velocity and acceleration supported the single-optimum OU model (AICc $w_{\text{singleOU}} = 0.830$, $w_{\text{Brownian motion}} = 0.169$, $w_{\text{micro}} = 0.001$). The microhabitat-based models were poorly supported in all tests (table 2),

Table 1: Evolutionary model comparison for morphological variables, analyzed across 191 species of anurans

Variable, model	K	ln L	AICc	ΔAICc	w_i
Relative leg length:					
Brownian motion	2	171.55	−339.03	8.56	.014
OU single optimum	3	171.59	−337.06	10.54	.005
Microhabitat	**8**	**182.19**	**−347.59**	**.00**	**.981**
Relative leg muscle mass:					
Brownian motion	2	−55.36	114.78	25.23	.000
OU single optimum	3	−50.16	106.46	16.91	.000
Microhabitat	**8**	**−36.38**	**89.55**	**.00**	**1.000**

Note: K is the number of parameters in each model. ln L is their log likelihood. AICc is the corrected Akaike information criterion. ΔAICc is the difference between a given model and the optimal model for a performance variable (that with the lowest AICc, shown in boldface). w_i are the AICc weights of models. OU = Ornstein-Uhlenbeck.

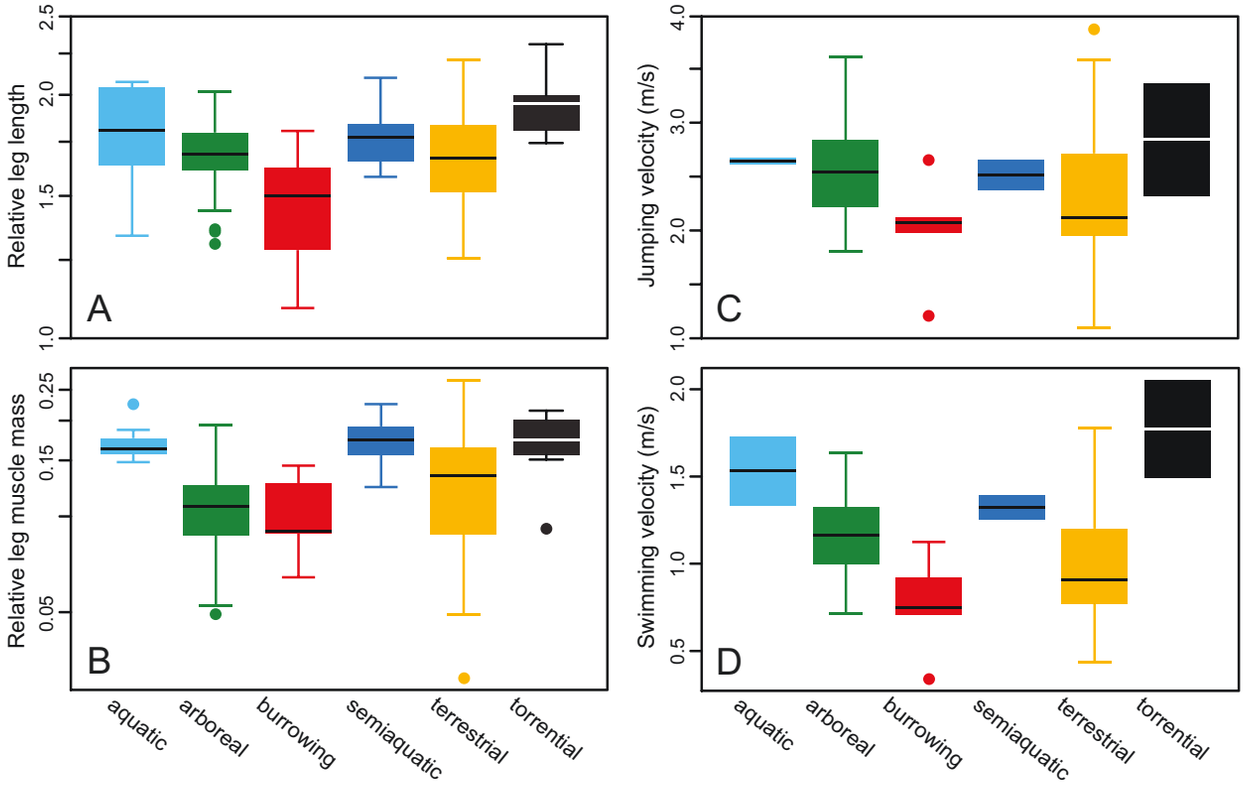

Figure 2: Boxplots of ecomorph differences in relative leg length (*A*), relative leg muscle mass (*B*), peak jumping velocity (*C*), and peak swimming velocity (*D*). In all plots, central lines of boxes give the median value across species. The upper and lower bounds of the boxes represent 75% and 25% quartiles, respectively. The whiskers represent 1.5 times the interquartile range (the height of the box) or the data extremes, whichever are closer to the median. Circles represent data outside the whisker range, if applicable. In the performance plots (*C*, *D*), three ecomorph categories only had two species each (aquatic, semiaquatic, and torrential), so the bounds of the boxes represent the actual values of the two species in each category. Note that the two morphological variables (*A*, *B*) are relative values and do not have units; they are plotted on a log scale. Performance variables (*C*, *D*) are in original units on a linear scale. While only velocity is presented here for performance, boxplots of jumping and swimming acceleration were similar.

and parametric bootstrapping simulations strongly supported all of these results (app. A).

Peak swimming velocity was best explained by a model that contrasted ecomorphs that regularly swim versus those that do not (table 2), with swimming ecomorphs having higher peak swimming velocity (table A5). The microhabitat model showed similar statistical support, likely because one of the nonswimming ecomorphs (burrowing) had lower peak swimming velocity than all other ecomorphs (fig. 2). Similarly, the swimming model was strongly favored for peak swimming acceleration (table 2), reflecting higher acceleration in the three swimming ecomorphs (table A5). Multivariate models of swimming velocity and acceleration gave similar results, with strong support for the swimming versus nonswimming ecomorph OU model (AICc $w_{swim} = 0.947$; AICc weights for all other models were each <0.04). As for morphology and jumping performance, bootstrapping simulations gave the same results (app. A). Finally, including the swimming ecomorph model in the jumping performance comparisons still showed the highest support for a single-optimum OU model (i.e., all ecomorphs have similar jumping performance), although this model was more weakly favored than before (table A6).

Testing the Fit between Leg Morphology and Performance

Most predictor variables were important for explaining variation in jumping and swimming peak velocity. For peak jumping velocity, the full model with all four variables (RLL, RLMM, body mass, and microhabitat) had the highest statistical support (table 3). Support for a model without body mass was slightly lower, while all other models had very low AICc weights (table 3). Results for peak swimming velocity were similar. The model with RLL, RLMM, and body mass

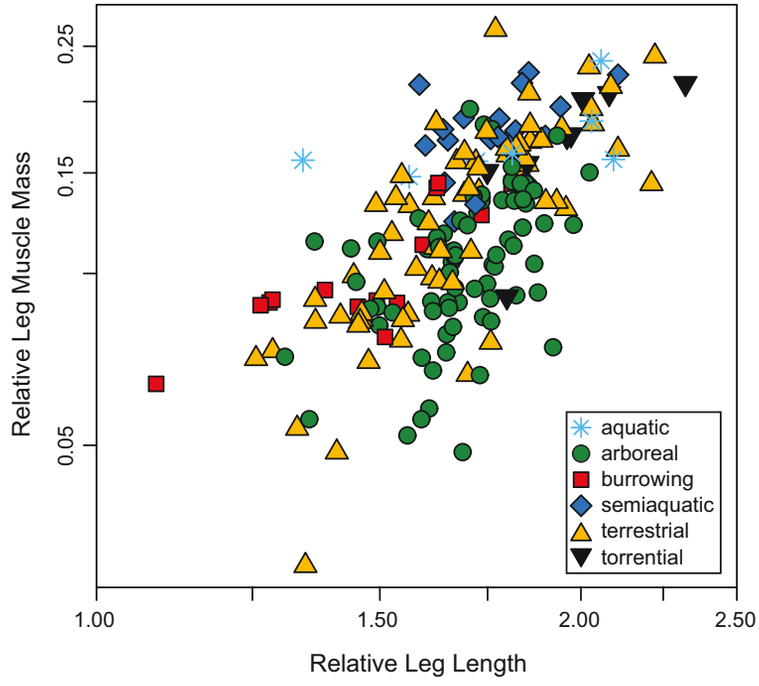

Figure 3: Plot of the correlation between relative leg length and relative leg muscle mass across 191 species of anurans. Variables are shown on a log scale in original units (i.e., ratio of leg length to body length; ratio of total leg muscle mass to total body mass). Mass and leg-length tick marks represent 0.05 and 0.25 units, respectively. Plotting these data as a phylomorphospace (fig. A2) shows the frequent convergence in morphology and ecology across species.

was most strongly supported, with the all-factor model having slightly lower support and no other models having appreciable support (table 4). For both jumping and swimming, the best-supported model explained more than 73% of the variation in peak velocity across species (tables 3, 4).

Comparing the importance of the two leg variables in jumping versus swimming could explain the link between high RLMM and high swimming performance in swimming ecomorphs. However, both RLL and RLMM were in all of the most strongly supported models for both jumping and swimming velocity, and both leg variables showed positive relationships with performance (fig. 4). Further analyses to tease apart the roles of the two variables gave similar results (see app. A for a detailed description of all methods and results). In particular, standard partial regression coefficients showed similar importance of RLL and RLMM in the most highly supported model of jumping velocity ($b_{\mathrm{RLL}} = 0.503$, $b_{\mathrm{RLMM}} = 0.491$) but a slightly higher importance of RLL over RLMM in the optimal model of swimming velocity ($b_{\mathrm{RLL}} = 0.515$, $b_{\mathrm{RLMM}} = 0.337$). In neither case was there evidence for trade-offs, which would be indicated by standard partial regression coefficients of differing sign. Overall, RLL and RLMM differed little in explaining variation across species in peak jumping and swimming velocity.

Discussion

In this article I analyzed the evolution of morphology and performance of anuran ecomorphs to understand their distinctive morphology. While previous articles have shown the distinct morphology (Moen et al. 2016) and performance (Moen et al. 2013) of these ecomorphs, these previous characterizations were made in multivariate morphological space and combined three aspects of performance into a single multivariate measure. Here I dissected the evolution of specific morphological characters that directly affect the performance of different behaviors, one important for all ecomorphs (jumping) and another especially important in only a subset (swimming). First, I found that across 191 species of frogs, ecomorphs were distinctive in leg morphology: burrowing species had relatively short legs for their body length and torrential species long legs (fig. 2*A*), and aquatic, semiaquatic, and torrential species had more muscular legs for their body mass than other ecomorphs (fig. 2*B*). Second, I found that jumping performance was largely conserved (fig. 2*C*) across ecomorphs, suggesting that selection maintains high jumping performance across most species of frogs. Yet swimming performance was not uniform, as it was higher in ecomorphs that regularly swim as adults (fig. 2*D*). Finally, I found that both RLL and

Table 2: Evolutionary model comparison for performance variables, analyzed across 44 species of anurans

Variable, model	K	ln L	AICc	ΔAICc	w_i
Jumping velocity:					
Brownian motion	2	−41.88	88.05	8.79	.011
OU single optimum	**3**	**−36.33**	**79.26**	**.00**	**.906**
Microhabitat	8	−31.96	84.03	4.78	.083
Jumping acceleration:					
Brownian motion	**2**	**−205.89**	**416.08**	**.00**	**.598**
OU single optimum	3	−205.14	416.88	.80	.401
Microhabitat	8	−204.20	428.51	12.43	.001
Swimming velocity:					
Brownian motion	2	−19.39	43.06	12.15	.001
OU single optimum	3	−15.76	38.11	7.20	.015
Swim in breeding	4	−15.72	40.46	9.55	.005
Swim regularly	**4**	**−10.94**	**30.91**	**.00**	**.559**
Microhabitat	8	−5.69	31.49	.57	.420
Swimming acceleration:					
Brownian motion	2	−163.19	330.68	7.80	.017
OU single optimum	3	−160.31	327.21	4.34	.097
Swim in breeding	4	−160.29	329.61	6.74	.029
Swim regularly	**4**	**−156.93**	**322.88**	**.00**	**.844**
Microhabitat	8	−155.51	331.14	8.26	.014

Note: K is the number of parameters in each model. ln L is their log likelihood. AICc is the corrected Akaike information criterion. ΔAICc is the difference between a given model and the optimal model for a performance variable (that with the lowest AICc, shown in boldface). w_i = the AICc weights of models. OU = Ornstein-Uhlenbeck.

RLMM independently affect both peak jumping and swimming velocity, that they do not show trade-offs in their effects on jumping and swimming performance, and that many morphologies can produce similar performance (fig. 4). These results are consistent with previous work (Alfaro et al. 2005; Thompson et al. 2017) showing that many morphological configurations produce similar functional output at intermediate levels of function, but very few combinations

Table 3: Relationship between predictor variables and jumping velocity across 44 species of anurans

Predictor	R^2	ln L	AICc	ΔAICc	w_i
Micro	−.031	−34.594	83.46	53.17	.000
RLMM	.464	−22.306	48.91	18.62	.000
RLL	.569	−17.881	40.05	9.76	.004
BM	.034	−35.362	75.02	44.73	.000
Micro + RLMM	.590	−14.489	46.09	15.80	.000
Micro + RLL	.568	−15.164	47.44	17.15	.000
Micro + BM	−.012	−33.496	84.10	53.81	.000
RLL + RLMM	**.615**	**−14.592**	**35.78**	**5.49**	**.035**
BM + RLMM	.455	−22.178	50.96	20.67	.000
BM + RLL	.566	−17.303	41.21	10.92	.002
Micro + RLL + RLMM	**.716**	**−5.422**	**30.96**	**.67**	**.394**
Micro + BM + RLMM	.585	−13.791	47.70	17.41	.000
Micro + BM + RLL	.593	−12.940	45.99	15.70	.000
BM + RLMM + RLL	.608	−14.380	37.78	7.50	.013
All factors	**.730**	**−3.498**	**30.29**	**.00**	**.550**

Note: R^2 is the adjusted R^2 of the model (the proportion of variation in the response variable explained by variation in the predictor variables). ln L is their log likelihood. AICc is the corrected Akaike information criterion. ΔAICc is the difference between a given model and the optimal model for a performance variable (that with the lowest AICc). w_i are the AICc weights of models. Boldfacing indicates highest-weight models that cumulatively represent 95% of the AICc weight. BM = body mass; micro = microhabitat; RLL = relative leg length; RLMM = relative leg muscle mass.

Table 4: Relationship between predictor variables and swimming velocity across 44 species of anurans

Predictor	R^2	ln L	AICc	ΔAICc	w_i
Micro	.238	−7.326	28.92	48.86	.000
RLMM	.530	1.025	2.24	22.18	.000
RLL	.609	4.832	−5.37	14.57	.000
BM	.030	−14.852	34.00	53.94	.000
Micro + RLMM	.677	11.622	−6.13	13.81	.001
Micro + RLL	.667	10.962	−4.81	15.13	.000
Micro + BM	.240	−6.728	30.57	50.51	.000
RLL + RLMM	.677	9.902	−13.20	6.74	.024
BM + RLMM	.520	1.113	4.37	24.32	.000
BM + RLL	.622	5.882	−5.16	14.78	.000
Micro + RLL + RLMM	**.775**	**20.028**	**−19.94**	**.00**	**.689**
Micro + BM + RLMM	.672	11.805	−3.50	16.45	.000
Micro + BM + RLL	.672	11.938	−3.76	16.18	.000
BM + RLMM + RLL	.674	10.192	−11.36	8.58	.009
All factors	**.778**	**20.700**	**−18.11**	**1.84**	**.275**

Note: R^2 is the adjusted R^2 of the model (the proportion of variation in the response variable explained by variation in the predictor variables). ln L is their log likelihood. AICc is the corrected Akaike information criterion. ΔAICc is the difference between a given model and the optimal model (that with the lowest AICc) for a performance variable. w_i are the AICc weights of models. Boldfacing indicates highest-weight models that cumulatively represent 95% of the AICc weight. BM = body mass; micro = microhabitat; RLL = relative leg length; RLMM = relative leg muscle mass.

of morphological values produce the highest output, although to my knowledge this is the first demonstration of this pattern in performance (rather than functional output calculated from morphological data or models). Nevertheless, while many-to-one mapping often permits frogs to achieve equivalent jumping velocity through having either particularly long legs (for a given muscle size) or particularly muscular legs (for a given leg length), the lack of trade-offs leaves it unclear why an ecomorph would have one morphology or the other. In other words, what determines the realized morphology of different ecomorphs?

What Explains the Characteristic Morphology of Anuran Ecomorphs?

The most distinctive pattern in leg morphology across ecomorphs was that aquatic, semiaquatic, and torrential species had high RLMM compared with the other three ecomorphs (fig. 2*B*). Since RLMM was positively correlated with RLL, this pattern could stem from swimming ecomorphs having more muscular legs for their leg length or just having overall longer legs. Figure 3 and the additional OU analysis of leg length–standardized leg muscle mass (table A4) show that in torrential species it is the latter pattern, whereas in aquatic and semiaquatic species it is the former. Given that these three ecomorphs had the highest peak swimming velocity and acceleration (fig. 2), I examined whether aquatic and semiaquatic species had higher leg muscle mass for their leg length because leg muscle mass was more important for swimming than leg length. Four different ways of evaluating this possibility gave no indication that this was the case. Moreover, because these ecomorphs have arisen many independent times (figs. 1, A2; Moen et al. 2016) and thus have convergently evolved their muscular legs, it is unlikely that shared ancestry or other contingent factors have led to their characteristic morphology.

Here I examined only RLL and RLMM to simplify the exploration of why frog ecomorphs have the distinctive morphology that they do, so the importance of leg muscle mass (over length) in swimming will require more detailed biomechanical study. Some evidence suggests that the mechanics of swimming varies across species (Johansson and Lauder 2004; Richards 2010; Robovska-Havelkova et al. 2014), and different ways to generate thrust map to different morphological characters (Richards 2010; Richards and Clemente 2013). A better understanding of variation in anuran swimming mechanics may thus be important for clearly addressing the importance of leg muscle mass in swimming frogs.

On the other hand, why might some taxa have long, thin legs? In particular, arboreal taxa have relatively low leg muscle mass for their leg length (table A4; fig. 3). It is possible that in this case, selection acts against high relative muscle mass as the way to achieve high jumping performance. Muscle is heavy tissue, and more muscular legs mean heavier legs, which will increase overall body mass. Such additional weight could limit species that regularly climb and maneuver in vertical habitats, but it may be less constraining to species frequently living in the water, where buoyancy reduces the constraint on having heavy bodies. Further analyses show that indeed arboreal taxa are lighter for their body length than

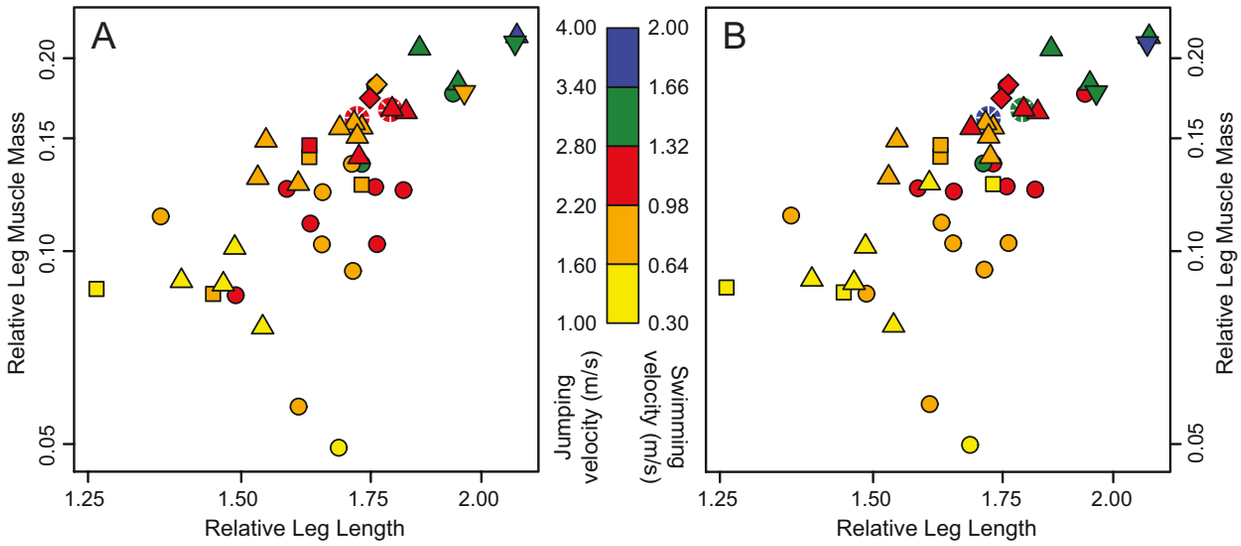

Figure 4: Relationships between relative leg length, relative leg muscle mass, and performance. Peak jumping velocity (*A*) and swimming velocity (*B*) are binned for easier visualization of patterns. Symbols represent the different ecomorphs as in figure 3: aquatic (white asterisks with a colored background that indicates performance), arboreal (circles), burrowing (squares), semiaquatic (diamonds), terrestrial (standard triangles), and torrential (upside-down triangles). Note that here, in contrast to all other figures, colors represent performance instead of ecomorph. Morphological variables are shown in original units on a log scale, while performance variables are shown in original units on a linear scale, following how these sets of variables were analyzed. The phylogenetic generalized least squares correlation between peak jumping and swimming velocity across species was 0.764, explaining the rough similarity between point colors in *A* and *B*.

aquatic and semiaquatic species. I conducted a PGLS regression of body mass on body length (SVL) and arboreal versus aquatic/semiaquatic microhabitat across the 191-species data set. This analysis showed that aquatic and semiaquatic species are 71.5% heavier than arboreal species at a given body length ($R^2 = 0.975$, $P < .001$; fig. A3). Interestingly, torrential species, which combine aspects of arboreal and aquatic life (e.g., they climb on streamside vegetation and wet rocks, and they dive into high-flow waters to swim to safety), generally fit between arboreal and aquatic/semiaquatic species (fig. A3). Future work will profitably examine the possible constraints of mass, particularly in legs, on vertical movement in frogs.

More generally, future research on the functional basis of ecomorphology in anurans will need to improve other limitations of this study. First, examining form-function relationships within ecomorph type was not possible in this study, given that there were too few species in many of the ecomorph categories (e.g., two each of aquatic, semiaquatic, and torrential species). Second, I examined the impact of only two morphological traits on the performance of two behaviors. The simplicity of this approach allowed me to address morphological evolution, performance evolution, and form-function relationships across many species and ecomorphs. Yet frog ecomorphs differ in many more traits than just leg length and leg muscle mass, including in toe webbing, toe pads, and head shape (Moen et al. 2013, 2016). Furthermore, differences in individual leg bones or muscles may occur among ecomorphs (Emerson 1976; Astley 2016). Thus, to further address the question of why frog ecomorphs have the morphology that they do, future studies should examine more species, from different clades and geographic regions, and other behaviors and morphological characters. Such an effort to better characterize the functional landscape of anurans will be substantial, partly given the logistical difficulty of obtaining performance data from clades distributed around the world, but also due to collecting such a diversity of data from many species.

Effects of Trade-Offs and Many-to-One Mapping on Macroevolution

Previous studies of the role of form-function relationships in macroevolution have focused on the relationship between many-to-one mapping and diversity or rates of evolution (Alfaro et al. 2004; Alfaro et al. 2005; Wainwright et al. 2005). Few studies have examined how many-to-one mapping may contrast with trade-offs in affecting macroevolution (e.g., Holzman et al. 2011). Two future areas of research seem particularly fruitful. First, many studies have examined rates of transition between different character states, increasingly at large scales (e.g., Gomez-Mestre et al. 2012; Pyron and Burbrink 2014; Zanne et al. 2014). Such rates are typically asymmetrical, yet little is known about what might cause such asymmetry. One possibility is that many-to-one mapping may facilitate such transitions. For example, both high leg muscle mass and long legs produce high jumping velocity, something beneficial for most anuran species

(Gans and Parsons 1966; Zug 1978). Moreover, arboreal frogs tend to have less muscular but longer legs, whereas aquatic and semiaquatic species have more muscular but shorter legs. Is it possible that transitions between arboreal and semiaquatic states are more frequent than others and that this happens because intermediate forms between these states would maintain high jumping velocity?

Second, while many morphological parts may affect a certain function, in reality some parts will affect that function more than others (Holzman et al. 2011; Anderson and Patek 2015). The function is thus more sensitive to evolutionary change in some parts than others, and since selection usually acts on function (Arnold 1983; Irschick et al. 2008), those influential parts may be more strongly constrained in macroevolution. Anderson and Patek (2015) showed that the links that most affected function of a four-bar mechanical system fit a model of stabilizing selection (OU model) to specific ecologies, as did the function. This suggested that those parts were constrained within a narrow range to maintain optimal function. However, subsequent studies of multiple four-bar systems showed that the most influential link had the highest rate of Brownian motion evolution (Muñoz et al. 2017, 2018), similar to a previous study (Holzman et al. 2012). Here I found many-to-one mapping in RLMM and RLL on both jumping and swimming performance. Moreover, both leg variables showed strong positive relationships with performance in both behaviors (tables 3, 4; fig. 4), suggesting that mechanics of jumping and swimming are equally sensitive to changes in both RLL and RLMM. Both leg variables fit a multipeak OU model (based on microhabitat/ecomorph), yet jumping and swimming velocity showed different macroevolutionary dynamics than morphology (table 2), clouding the link between the macroevolutionary dynamics of leg morphology and functional performance. A more detailed examination of the morphology that affects each behavior (e.g., foot webbing area and shape, more detailed muscle dissection; see above) may reveal that many more parts affect the functions but that only some are driving their evolution.

Conclusions

Many explanations for ecomorphology are based on relatively simplistic characterizations of morphology, and links to function (and thus selection) are anecdotal. When mapping morphology to performance in multiple behaviors, however, trade-offs and many-to-one mapping may obscure the fit between ecology, form, and function. Here I considered two morphological variables that affect performance in two behaviors across six ecomorphs. I found that swimming ecomorphs have higher swimming performance and more muscular legs than nonswimming ecomorphs while having similar jumping performance as other ecomorphs. By contrast, other ecomorphs may not have legs as muscular as swimming ecomorphs possibly due to trade-offs with other unmeasured behaviors (e.g., climbing), but they achieve similar jumping performance by having relatively long legs. This many-to-one mapping alleviates potential trade-offs between jumping (a shared behavior) and other behaviors, and it allows species to have specialized morphology related to nonjumping behaviors. Overall, my comparative phylogenetic approach can be extended to other organisms to better understand the roles of multiple behaviors on the distinctive morphology associated with ecology in groups that show ecomorphology.

Acknowledgments

I thank Dalton Hanson for help with preliminary analyses and Sheila Patek and Phil Anderson for discussions that improved my thinking about this article. I also thank Daniel Bolnick, Robert Dudley, and two anonymous reviewers for constructive comments on the article. A National Science Foundation grant (DEB-1655812) partly supported the preparation of the manuscript and also supported the Oklahoma State University High-Performance Computing Center (OCI-1126330), at which I conducted some analyses for this article. No conflicts of interest have influenced this work.

Literature Cited

Adams, D. C., and M. L. Collyer. 2018. Multivariate phylogenetic comparative methods: evaluations, comparisons, and recommendations. Systematic Biology 67:14–31.

Alfaro, M. E., D. I. Bolnick, and P. C. Wainwright. 2004. Evolutionary dynamics of complex biomechanical systems: an example using the four-bar mechanism. Evolution 58:495–503.

———. 2005. Evolutionary consequences of many-to-one mapping of jaw morphology to mechanics in labrid fishes. American Naturalist 165:E140–E154.

Anderson, P. S., and S. N. Patek. 2015. Mechanical sensitivity reveals evolutionary dynamics of mechanical systems. Proceedings of the Royal Society B 282:20143088.

Arakaki, M., P.-A. Christin, R. Nyffeler, A. Lendel, U. Eggli, R. M. Ogburn, E. Spriggs, M. J. Moore, and E. J. Edwards. 2011. Contemporaneous and recent radiations of the world's major succulent plant lineages. Proceedings of the National Academy of Sciences of the USA 108:8379–8384.

Arnold, S. J. 1983. Morphology, performance and fitness. American Zoologist 23:347–361.

Astley, H. C. 2016. The diversity and evolution of locomotor muscle properties in anurans. Journal of Experimental Biology 219:3163–3173.

Bergmann, P. J., and E. J. McElroy. 2014. Many-to-many mapping of phenotype to performance: an extension of the F-matrix for studying functional complexity. Evolutionary Biology 41:546–560.

Boettiger, C., G. Coop, and P. Ralph. 2012. Is your phylogeny informative? measuring the power of comparative methods. Evolution 66:2240–2251.

Bossuyt, F., and M. C. Milinkovitch. 2000. Convergent adaptive radiations in Madagascan and Asian ranid frogs reveal covariation between larval and adult traits. Proceedings of the National Academy of Sciences of the USA 97:6585–6590.

Burnham, K. P., and D. R. Anderson. 2002. Model selection and multimodel inference: a practical information-theoretic approach. Springer, New York.

Butler, M. A., and A. A. King. 2004. Phylogenetic comparative analysis: a modeling approach for adaptive evolution. American Naturalist 164:683–695.

Careau, V., P. A. Biro, C. Bonneaud, E. B. Fokam, and A. Herrel. 2014. Individual variation in thermal performance curves: swimming burst speed and jumping endurance in wild-caught tropical clawed frogs. Oecologia 175:471–480.

Choi, I.-H., and K. Park. 1996. Variations in take-off velocity of anuran amphibians: relation to morphology, muscle contractile function, and enzyme activity. Comparative Biochemistry and Physiology 113A:393–400.

Choi, I.-H., J. H. Shim, and R. E. Ricklefs. 2003. Morphometric relationships of take-off speed in anuran amphibians. Journal of Experimental Zoology A 299:99–102.

Citadini, J. M., R. Brandt, C. R. Williams, and F. R. Gomes. 2018. Evolution of morphology and locomotor performance in anurans: relationships with microhabitat diversification. Journal of Evolutionary Biology 31:371–381.

Duellman, W. E., and L. Trueb. 1986. Biology of amphibians. Johns Hopkins University Press, Baltimore.

Emerson, S. B. 1976. Burrowing in frogs. Journal of Morphology 149:437–458.

———. 1978. Allometry and jumping in frogs: helping the twain to meet. Evolution 32:551–564.

———. 1979. The ilio-sacral articulation in frogs: form and function. Biological Journal of the Linnean Society 11:153–168.

———. 1988. Convergence and morphological constraint in frogs: variation in postcranial morphology. Fieldiana Zoology 43:1–19.

Endler, J. A. 1995. Multiple-trait coevolution and environmental gradients in guppies. Trends in Ecology and Evolution 10:22–29.

FitzJohn, R. G. 2012. diversitree: comparative phylogenetic analyses of diversification in R. Methods in Ecology and Evolution 3:1084–1092.

Freckleton, R. P., P. H. Harvey, and M. Pagel. 2002. Phylogenetic analysis and comparative data: a test and review of evidence. American Naturalist 160:712–726.

Gal, J. M., and R. W. Blake. 1987. Hydrodynamic drag of two frog species: *Hymenochirus boettgeri* and *Rana pipiens*. Canadian Journal of Zoology 65:1085–1090.

———. 1988. Biomechanics of frog swimming. I. Estimation of the propulsive force generated by *Hymenochirus boettgeri*. Journal of Experimental Biology 138:399–411.

Gans, C., and T. S. Parsons. 1966. On the origin of the jumping mechanism in frogs. Evolution 20:92–99.

Gillis, G. B., and A. A. Biewener. 2000. Hindlimb extensor muscle function during jumping and swimming in the toad (*Bufo marinus*). Journal of Experimental Biology 203:3547–3563.

Gomes, F. R., E. L. Rezende, M. B. Grizante, and C. A. Navas. 2009. The evolution of jumping performance in anurans: morphological correlates and ecological implications. Journal of Evolutionary Biology 22:1088–1097.

Gomez-Mestre, I., R. A. Pyron, and J. J. Wiens. 2012. Phylogenetic analyses reveal unexpected patterns in the evolution of reproductive modes in frogs. Evolution 66:3687–3700.

Haddad, C. F. B., and C. P. d. A. Prado. 2005. Reproductive modes in frogs and their unexpected diversity in the Atlantic forest of Brazil. Bioscience 55:207–217.

Hansen, T. F. 1997. Stabilizing selection and the comparative analysis of adaptation. Evolution 51:1341–1351.

Hansen, T. F., and S. H. Orzack. 2005. Assessing current adaptation and phylogenetic inertia as explanations of trait evolution: the need for controlled comparisons. Evolution 59:2063–2072.

Holzman, R., D. C. Collar, R. S. Mehta, and P. C. Wainwright. 2011. Functional complexity can mitigate performance trade-offs. American Naturalist 177:E69–E83.

Holzman, R., D. C. Collar, S. A. Price, C. D. Hulsey, R. C. Thomson, and P. C. Wainwright. 2012. Biomechanical trade-offs bias rates of evolution in the feeding apparatus of fishes. Proceedings of the Royal Society B 279:1287–1292.

Huelsenbeck, J. P., R. Nielsen, and J. P. Bollback. 2003. Stochastic mapping of morphological characters. Systematic Biology 52:131–158.

Irschick, D. J., J. J. Meyers, J. F. Husak, and J.-F. le Galliard. 2008. How does selection operate on whole-organism functional performance capacities? a review and synthesis. Evolutionary Ecology Research 10:177–196.

James, R. S., C. A. Navas, and A. Herrel. 2007. How important are skeletal muscles in setting limits on jumping performance? Journal of Experimental Biology 210:923–933.

James, R. S., and R. S. Wilson. 2008. Explosive jumping: extreme morphological and physiological specializations of Australian rocket frogs (*Litoria nasuta*). Physiological and Biochemical Zoology 81:176–185.

Johansson, L. C., and G. V. Lauder. 2004. Hydrodynamics of surface swimming in leopard frogs (*Rana pipiens*). Journal of Experimental Biology 207:3945–3958.

King, A. A., and M. A. Butler. 2009. ouch: Ornstein-Uhlenbeck models for phylogenetic comparative hypotheses. R package version 1.1-3.

Koehl, M. A. R. 1996. When does morphology matter? Annual Review of Ecology and Systematics 27:501–542.

Losos, J. B. 1990. Ecomorphology, performance capability, and scaling of West Indian *Anolis* lizards: an evolutionary analysis. Ecological Monographs 60:369–388.

———. 2011. Convergence, adaptation, and constraint. Evolution 65:1827–1840.

Lutz, G. J., and L. C. Rome. 1994. Built for jumping: the design of the frog muscular system. Science 263:370–372.

Marks, C. O., and M. J. Lechowicz. 2006. Alternative designs and the evolution of functional diversity. American Naturalist 167:55–66.

Marsh, R. L. 1994. Jumping ability of anuran amphibians. Pages 51–111 *in* J. H. Jones, ed. Advances in veterinary science and comparative medicine. Academic Press, New York.

Marsh, R. L., and H. B. John-Alder. 1994. Jumping performance of hylid frogs measured with high-speed cine film. Journal of Experimental Biology 188:131–141.

Martins, E. P., and T. F. Hansen. 1997. Phylogenies and the comparative method: a general approach to incorporating phylogenetic information into the analysis of interspecific data. American Naturalist 149:646–667.

Melville, J., L. J. Harmon, and J. B. Losos. 2006. Intercontinental community convergence of ecology and morphology in desert lizards. Proceedings of the Royal Society B 273:557–563.

Moen, D. S. 2019. Data from: What determines the distinct morphology of species with a particular ecology? the roles of many-to-one mapping and trade-offs in the evolution of frog ecomorphology and performance. American Naturalist, Dryad Digital Repository, http://doi.org/10.5061/dryad.n07742q.

Moen, D. S., D. J. Irschick, and J. J. Wiens. 2013. Evolutionary conservatism and convergence both lead to striking similarity in ecology,

morphology and performance across continents in frogs. Proceedings of the Royal Society B 280:20132156.
Moen, D. S., H. Morlon, and J. J. Wiens. 2016. Testing convergence versus history: convergence dominates phenotypic evolution for over 150 million years in frogs. Systematic Biology 65:146–160.
Moen, D. S., and J. J. Wiens. 2017. Microhabitat and climatic niche change explain patterns of diversification among frog families. American Naturalist 190:29–44.
Muñoz, M. M., P. S. Anderson, and S. N. Patek. 2017. Mechanical sensitivity and the dynamics of evolutionary rate shifts in biomechanical systems. Proceedings of the Royal Society B 284:20162325.
Muñoz, M. M., Y. Hu, P. S. L. Anderson, and S. N. Patek. 2018. Strong biomechanical relationships bias the tempo and mode of morphological evolution. eLife 7:e37621.
Muschick, M., A. Indermaur, and W. Salzburger. 2012. Convergent evolution within an adaptive radiation of cichlid fishes. Current Biology 22:2362–2368.
Nauwelaerts, S., and P. Aerts. 2003. Propulsive impulse as a covarying performance measure in the comparison of the kinematics of swimming and jumping in frogs. Journal of Experimental Biology 206:4341–4351.
Nauwelaerts, S., J. Ramsay, and P. Aerts. 2007. Morphological correlates of aquatic and terrestrial locomotion in a semi-aquatic frog, *Rana esculenta*: no evidence for a design conflict. Journal of Anatomy 210:304–317.
Navas, C. A., F. R. Gomes, and J. E. Carvalho. 2008. Thermal relationship and exercise physiology in anuran amphibians: integration and evolutionary implications. Comparative Biochemistry and Physiology 151A:344–362.
Orme, C. D. L., R. P. Freckleton, G. H. Thomas, T. Petzoldt, S. A. Fritz, N. Isaac, and W. Pearse. 2013. caper: comparative analyses of phylogenetics and evolution using R, version 0.5.2.
Pagel, M. 1997. Inferring evolutionary processes from phylogenies. Zoologica Scripta 26:331–348.
Parker, G. A., and J. Maynard Smith. 1990. Optimality theory in evolutionary biology. Nature 348:27–33.
Pélabon, C., C. Firmat, G. H. Bolstad, K. L. Voje, D. Houle, J. Cassara, A. L. Rouzic, and T. F. Hansen. 2014. Evolution of morphological allometry. Annals of the New York Academy of Sciences 1320:58–75.
Peters, S. E., L. T. Kamel, and D. P. Bashor. 1996. Hopping and swimming in the leopard frog, *Rana pipiens*. I. Step cycles and kinematics. Journal of Morphology 230:1–16.
Pyron, R. A. 2014. Biogeographic analysis reveals ancient continental vicariance and recent oceanic dispersal in amphibians. Systematic Biology 63:779–797.
Pyron, R. A., and F. T. Burbrink. 2014. Early origin of viviparity and multiple reversions to oviparity in squamate reptiles. Ecology Letters 17:13–21.
Pyron, R. A., and J. J. Wiens. 2011. A large-scale phylogeny of Amphibia including over 2800 species, and a revised classification of extant frogs, salamanders, and caecilians. Molecular Phylogenetics and Evolution 61:543–583.
Revell, L. J. 2010. Phylogenetic signal and linear regression on species data. Methods in Ecology and Evolution 1:319–329.
———. 2012. phytools: an R package for phylogenetic comparative biology (and other things). Methods in Ecology and Evolution 3:217–223.
Reynaga, C. M., H. C. Astley, and E. Azizi. 2018. Morphological and kinematic specializations of walking frogs. Journal of Experimental Zoology A 329:87–98.
Richards, C. T. 2010. Kinematics and hydrodynamics analysis of swimming anurans reveals striking inter-specific differences in the mechanism for producing thrust. Journal of Experimental Biology 213:621–634.
Richards, C. T., and C. J. Clemente. 2013. Built for rowing: frog muscle is tuned to limb morphology to power swimming. Journal of the Royal Society Interface 10:20130236.
Robinson, B. W., and D. S. Wilson. 1998. Optimal foraging, specialization, and a solution to Liem's paradox. American Naturalist 151:223–235.
Robovska-Havelkova, P., P. Aerts, Z. Rocek, T. Prikryl, A. C. Fabre, and A. Herrel. 2014. Do all frogs swim alike? the effect of ecological specialization on swimming kinematics in frogs. Journal of Experimental Biology 217:3637–3644.
Rohlf, F. J. 2006. A comment on phylogenetic correction. Evolution 60:1509–1515.
Scales, J. A., and M. A. Butler. 2016. Adaptive evolution in locomotor performance: how selective pressures and functional relationships produce diversity. Evolution 70:48–61.
Shubin, N. H., and F. A. J. Jenkins. 1995. An early Jurassic jumping frog. Nature 377:49–52.
Sokal, R. R., and F. J. Rohlf. 1995. Biometry. W. H. Freeman, New York.
Thompson, C. J., N. I. Ahmed, T. Veen, C. L. Peichel, A. P. Hendry, D. I. Bolnick, and Y. E. Stuart. 2017. Many-to-one form-to-function mapping weakens parallel morphological evolution. Evolution 71:2738–2749.
Wainwright, P. C. 2007. Functional versus morphological diversity in macroevolution. Annual Review of Ecology, Evolution, and Systematics 38:381–401.
Wainwright, P. C., M. E. Alfaro, D. I. Bolnick, and C. D. Hulsey. 2005. Many-to-one mapping of form to function: a general principle in organismal design? Integrative and Comparative Biology 45:256–262.
Wainwright, P. C., and S. M. Reilly. 1994. Ecological morphology: integrative organismal biology. University of Chicago Press, Chicago.
Walker, J. A. 1998. Estimating velocities and accelerations of animal locomotion: a simulation experiment comparing numerical differentiation algorithms. Journal of Experimental Biology 201:981–995.
———. 2007. A general model of functional constraints on phenotypic evolution. American Naturalist 170:681–689.
Wilson, R. S. 2001. Geographic variation in thermal sensitivity of jumping performance in the frog *Limnodynastes peronii*. Journal of Experimental Biology 204:4227–4236.
Winemiller, K. O. 1991. Ecomorphological diversification in lowland freshwater fish assemblages from five biotic regions. Ecological Monographs 61:343–365.
Zanne, A. E., D. C. Tank, W. K. Cornwell, J. M. Eastman, S. A. Smith, R. G. FitzJohn, D. J. McGlinn, et al. 2014. Three keys to the radiation of angiosperms into freezing environments. Nature 506:89–92.
Zug, G. R. 1978. Anuran locomotion: structure and function. 2. Jumping performance of semiaquatic, terrestrial, and arboreal frogs. Smithsonian Contributions to Zoology 276:1–31.

References Cited Only in the Online Enhancements

AmphibiaWeb. 2016. Information on amphibian biology and conservation. Accessed September 15, 2016. http://amphibiaweb.org.
Beaulieu, J. M., D. C. Jhwueng, C. Boettiger, and B. C. O'Meara. 2012. Modeling stabilizing selection: expanding the Ornstein-Uhlenbeck model of adaptive evolution. Evolution 66:2369–2383.

Blackburn, D. C., and W. E. Duellman. 2013. Brazilian marsupial frogs are diphyletic (Anura: Hemiphractidae: *Gastrotheca*). Molecular Phylogenetics and Evolution 68:709–714.

Bollback, J. P. 2005. Posterior mapping and posterior predictive distributions. Pages 180–203 *in* R. Nielsen, ed. Statistical methods in molecular evolution. Springer, New York.

———. 2006. SIMMAP: stochastic character mapping of discrete traits on phylogenies. BMC Bioinformatics 7:88.

Cooper, N., G. H. Thomas, C. Venditti, A. Meade, and R. P. Freckleton. 2016. A cautionary note on the use of Ornstein-Uhlenbeck models in macroevolutionary studies. Biological Journal of the Linnean Society 118:64–77.

Cressler, C. E., M. A. Butler, and A. A. King. 2015. Detecting adaptive evolution in phylogenetic comparative analysis using the Ornstein-Uhlenbeck model. Systematic Biology 64:953–968.

Davis, M., P. E. Midford, and W. P. Maddison. 2013. Exploring power and parameter estimation of the BiSSE method for analyzing species diversification. BMC Evolutionary Biology 13:38.

Frost, D. R. 2016. Amphibian species of the world: an online reference, version 6.0. Accessed October 29, 2016. American Museum of Natural History, New York. http://research.amnh.org/herpetology/amphibia/index.html.

García-Berthou, E. 2001. On the misuse of residuals in ecology: testing regression residuals vs. the analysis of covariance. Journal of Animal Ecology 70:708–711.

Garland, T. J., A. W. Dickerman, C. M. Janis, and J. A. Jones. 1993. Phylogenetic analysis of covariance by computer simulation. Systematic Biology 42:265–292.

Ghalambor, C. K., J. A. Walker, and D. A. Reznick. 2003. Multi-trait selection, adaptation, and constraints on the evolution of burst swimming performance. Integrative and Comparative Biology 43:431–438.

Hansen, T. F. 2014. Use and misuse of comparative methods in the study of adaptation. Pages 351–379 *in* L. Z. Garamszegi, ed. Modern phylogenetic comparative methods and their application in evolutionary biology. Springer, Berlin.

Hansen, T. F., J. Pienaar, and S. H. Orzack. 2008. A comparative method for studying adaptation to a randomly evolving environment. Evolution 62:1965–1977.

Hedges, S. B., W. E. Duellman, and M. P. Heinicke. 2008. New World direct-developing frogs (Anura: Terrarana): molecular phylogeny, classification, biogeography, and conservation. Zootaxa 1737:1–182.

Ho, L. S. T., and C. Ané. 2014. Intrinsic inference difficulties for trait evolution with Ornstein-Uhlenbeck models. Methods in Ecology and Evolution 5:1133–1146.

Houle, D., C. Pélabon, G. Wagner, and T. F. Hansen. 2011. Measurement and meaning in biology. Quarterly Review of Biology 86:3–34.

IUCN (International Union for Conservation of Nature). 2014. The IUCN Red List of Threatened Species. Version 2014. Accessed September 15, 2016. http://www.iucnredlist.org.

Johnson, J. B., and K. S. Omland. 2004. Model selection in ecology and evolution. Trends in Ecology and Evolution 19:101–108.

Maddison, W. P., P. E. Midford, and S. P. Otto. 2007. Estimating a binary character's effect on speciation and extinction. Systematic Biology 56:701–710.

Manly, B. F. J. 1994. Multivariate statistical methods: a primer. Chapman & Hall, London.

O'Meara, B. C., and J. M. Beaulieu. 2014. Modelling stabilizing selection: the attraction of Ornstein-Uhlenbeck models. Pages 381–393 *in* L. Z. Garamszegi, ed. Modern phylogenetic comparative methods and their application in evolutionary biology. Springer, Berlin.

Packard, G. C., and T. J. Boardman. 1988. The misuse of ratios, indices, and percentages in ecophysiological research. Physiological Zoology 61:1–9.

Pagel, M. 1999. The maximum likelihood approach to reconstructing ancestral character states of discrete characters on phylogenies. Systematic Biology 48:612–622.

Posada, D., and T. R. Buckley. 2004. Model selection and model averaging in phylogenetics: advantages of Akaike information criterion and Bayesian approaches over likelihood ratio tests. Systematic Biology 53:793–808.

Revell, L. J. 2009. Size-correction and principal components for interspecific comparative studies. Evolution 63:3258–3268.

———. 2013. A comment on the use of stochastic character maps to estimate evolutionary rate variation in a continuously valued trait. Systematic Biology 62:339–345.

Sá, R. O. d., T. Grant, A. Camargo, W. R. Heyer, M. L. Ponssa, and E. Stanley. 2014. Systematics of the Neotropical genus *Leptodactylus* Fitzinger, 1826 (Anura: Leptodactylidae): phylogeny, the relevance of non-molecular evidence, and species accounts. South American Journal of Herpetology 9:S1–S100.

Wiens, J. J., C. A. Kuczynski, X. Hua, and D. S. Moen. 2010. An expanded phylogeny of treefrogs (Hylidae) based on nuclear and mitochondrial sequence data. Molecular Phylogenetics and Evolution 55:871–882.

Wollenberg, K. C., D. R. Vieites, F. Glaw, and M. Vences. 2011. Speciation in little: the role of range and body size in the diversification of Malagasy mantellid frogs. BMC Evolutionary Biology 11:217.

Zar, J. H. 1999. Biostatistical analysis. Prentice Hall, Upper Saddle River, NJ.

Zimkus, B. M., and S. Schick. 2010. Light at the end of the tunnel: insights into the molecular systematics of East African puddle frogs (Anura: Phrynobatrachidae). Systematics and Biodiversity 8:39–47.

Associate Editor: Robert Dudley
Editor: Daniel I. Bolnick

 DOI: 10.1086/704736

Appendix A from D. S. Moen, "What Determines the Distinct Morphology of Species with a Particular Ecology? The Roles of Many-to-One Mapping and Trade-Offs in the Evolution of Frog Ecomorphology and Performance" (Am. Nat., vol. 194, no. 4, p. E000)

Supplementary Statistical Methods and Results

Reclassifying Microhabitat Use

I herein reclassify four species from Moen et al. (2013), using the same literature sources for microhabitat use but reinterpreted in light of more recent anuran ecomorph studies (Moen et al. 2016; Moen and Wiens 2017): *Amolops tuberodepressus* as torrential, *Odorrana grahami* as torrential, *Litoria dahlii* as aquatic, and *Chiasmocleis bassleri* as semiburrowing (partly burrowing, partly terrestrial). Despite these changes, for the current analyses I consider *C. bassleri* as originally classified (terrestrial), given that this study does not focus on burrowing taxa. That is, lumping *C. bassleri* with either burrowing or terrestrial taxa should have little qualitative effect on the results, given my emphasis on jumping (important for all taxa) and swimming (important for some; see below). None of the species from Moen et al. (2016) needed to be reclassified for microhabitat use.

Using Ratios to Size Standardize Variables

In this article, I use ratios to standardize variables to body size. A key advantage of using ratios instead of alternatives (see below) is that one can directly link variation in a functionally important variable (e.g., how long are legs relative to body length) to performance. Moreover, one can visually assess patterns in a biologically meaningful way (e.g., one can see how much jumping velocity increases when a frog has 33% longer legs and 50% more muscle mass in its legs compared with another species; fig. 4).

In some cases use of ratios may not be statistically optimal. For example, when multiple predictor variables are used to explain variation in a single response variable, ratios can be statistically inferior to including raw variables (here, leg length and leg muscle mass) and the standardization variable (here, body size) together as predictor variables in a general linear model (García-Berthou 2001). However, I use ratios here for three reasons. First, my standardization variable depended on the predictor variable (leg muscle mass standardized by preserved body mass; leg length standardized by body length [snout-to-vent length]), so it would be inappropriate to use a single standardization variable (live mass, preserved mass, or body length) in a combined regression. Here biological meaning (accurate standardization as it relates to functional performance) is favored over statistical ideals (Houle et al. 2011; Hansen 2014). Second, my estimate of body size as it affects performance in my regression models (live total body mass) is also different from the standardization variables. Third, statistical problems of using ratios as data primarily stem from (1) undesirable numerical properties of ratios (Sokal and Rohlf 1995) and (2) allometry between the numerator and denominator that leads to incomplete standardization (Packard and Boardman 1988).

Of these statistical problems, the first is empirical and does not characterize my data (e.g., because the denominators are continuous, the ratios are not limited to certain values; my data are far from the lower bound of 0.0 and either unbounded [relative leg length, or RLL] or far from the upper bound of 1.0 [relative leg muscle mass, or RLMM]). Second, I tested allometry between leg variables and their standardization variables by conducting phylogenetic generalized least squares (PGLS) regression (Martins and Hansen 1997) with λ taking its maximum likelihood value (Pagel 1997; Freckleton et al. 2002; Revell 2010). These analyses showed that relationships were nearly always isometric for both leg variables across both the 191- and the 44-species data set (table A1; fig. A1), which means that ratios are not a function of size. Nonetheless, residuals could be used for size standardization instead of ratios (Revell 2009). I considered this possibility and found strong correlations between residuals from the analyses described above and their corresponding ratios, ranging from 0.942 to 0.999. Moreover, I replicated key analyses with these

residuals as data and found that the results were almost quantitatively identical to those obtained with ratios (results not shown). Thus, I retain the use of ratios to facilitate biological interpretation of my results, as described above.

Assigning Internal States for Ornstein-Uhlenbeck (OU) Models

Current implementations of OU models require assigning internal branches to a fixed state (in this case, a microhabitat state). As in a previous study of anuran morphological evolution (Moen et al. 2016), I considered three possible ways to assign states to internal branches, all of which gave similar results (see below).

In the first approach, I compared three models of microhabitat-use evolution: equal rates (all transitions between states have the same rates), symmetric (rates between two particular states are the same but different from other states), and all rates different (each transition has its own rate). The likelihood of each model was estimated in the R package diversitree (ver. 0.9-9; FitzJohn 2012) assuming no effect of character states on diversification (Maddison et al. 2007; FitzJohn 2012), given that these phylogenies are far too sparsely sampled to accurately estimate such effects (Davis et al. 2013). I used the Akaike information criterion corrected for small sample sizes (AICc; Burnham and Anderson 2002) to compare models, and the symmetric model had the lowest AICc for the 191-species morphological data set (symmetric AICc $=$ 420.7 $<$ equal-rates AICc $=$ 438.4 $<$ all-rates-different AICc $=$ 446.1). In the 44-species performance data set, the equal-rates model had the lowest AICc for microhabitat (equal-rates AICc $=$ 109.2 $<$ symmetric AICc $=$ 140.2 $<$ all-rates-different AICc $=$ 291.1). The water breeding (vs. not) and swimming ecomorph (vs. not) models were binary, so I considered only symmetric and asymmetric models (also called single- and two-rate models). For water breeding the asymmetric model was favored (symmetric AICc $=$ 35.8, asymmetric AICc $=$ 33.5), while for swimming ecomorphs it was the symmetric model (symmetric AICc $=$ 30.8, asymmetric AICc $=$ 33.0).

I then used the optimal model and its maximum likelihood rate estimates to calculate marginal likelihood support for states at the internal nodes. Most nodes were strongly supported as being a particular state (e.g., 150 of 190 nodes in the 191-species data set, with "strong support" defined as being 7.39 times more likely than the state with the second-highest likelihood; Pagel 1999). Finally, at each node I assigned the state with the highest likelihood as the internal state for fitting OU models (i.e., the branch subtending each node was assigned its node's state).

Given that 40 of the nodes were uncertain in the 191-species data set, a second approach would be to use diversitree's joint ancestral state estimation procedure, which gives the single-state mapping at all nodes that has the highest likelihood. The benefit of such an approach is that it provides a single state at every node; however, I found this procedure to occasionally give unusual results (e.g., assigning a state in a part of the tree where that state is otherwise completely absent) and thus did not use it. Regardless, using marginal state estimates and choosing the state with the highest likelihood at each node (as above) gave nearly identical results as the joint approach, possibly because the two approaches estimated different states at only nine of 190 nodes (results not shown).

As a third approach, I estimated ancestral states using Bayesian stochastic character mapping (Huelsenbeck et al. 2003; Bollback 2005, 2006) with phytools version 0.5-20 (Revell 2012). This method has the advantage of integrating over uncertainty in internal state estimates when fitting OU models, and it allows states to change along branches instead of only at nodes. However, rates of transition among microhabitats are high in frogs (Moen et al. 2016), and such high rates can lead to error in stochastic mapping simulation replicates, which then leads to error in downstream analyses that depend on these internal states (Revell 2013). Thus, I did not use these mappings as my primary method of assigning internal states for OU models. However, I tested the sensitivity of my results to this decision by also analyzing OU models in which I used stochastic character mapping to determine internal states. I did this for a subset of my data to examine the sensitivity of results for one variable at a large tree size (RLMM; 191 species) and one variable at the smaller tree size (swimming velocity; 44 species).

In the case of RLMM, I tested among three possible models: Brownian motion, single-optimum OU, and microhabitat-specific OU (see the main text). Only the last of these models necessitates specifying internal states, for which I used the simmap (e.g., "make.simmap") commands in phytools. I used all default options to create 100 stochastic character maps of microhabitat evolution under the maximum likelihood model of transition rates (the symmetric model; see above). Then, for each of these maps I optimized a microhabitat-based OU model of RLMM evolution using the R package OUwie (Beaulieu et al. 2012), as ouch does not accommodate stochastic character maps. Finally, I compared models across stochastic character map replicates. I did this in two ways. First, I calculated the AICc weights of Brownian motion, single-optimum OU, and microhabitat-based OU for each replicate, and I calculated the mean and standard error of these weights across replicates. Second, I compared how frequently (across the 100 mapping replicates) each of the

three models of evolution was ranked first, second, or third in model fit. For RLMM evolution across 191 species, stochastic character mapping gave qualitatively identical results as the analyses presented in the main text (table A7; fig. A4), with the microhabitat model strongly favored.

In analyses of swimming velocity, there were two additional models that required specifying internal states: the swimming ecomorph model (adults typically swim or not) and the breeding model (the species breeds in the water or not). Given that my primary analyses showed no support for the breeding model, I here considered only the swimming model. Thus, I repeated the above stochastic character mapping analyses on the 44-species tree to estimate internal states for both the swimming model and the microhabitat model. I simulated 100 maps, using the default options in phytools and using the optimal model of character-state transition (equal-rates model for microhabitat and single-rate model for swimming ecomorph; see above). As for the 191-species tree, I compared models across stochastic map replicates by (1) calculating means and standard errors of AICc weights across replicates and (2) comparing model ranks across replicates. I found results similar to those in the main analyses (table A7; fig. A4), which showed strongest support for the swimming ecomorph model, with the microhabitat model less favored but also showing high support (table 2).

Using Parametric Bootstrapping to Calculate Statistical Significance and Power

Using OU models to study adaptive evolution over macroevolutionary timescales has been both promoted and criticized in recent years. These models are conceptually and statistically the most appropriate ones to use for the questions I pose in this article (Hansen 1997; Butler and King 2004; Hansen and Orzack 2005; Hansen et al. 2008; Hansen 2014), particularly when one is analyzing the adaptation of a continuous character in response to a discrete ecological factor (e.g., habitat, diet). The most commonly used alternative method in this case, a Brownian motion-based phylogenetic ANOVA or MANOVA (Garland et al. 1993), is not appropriate because the discrete selective regime is implicitly assumed to be constant for the entire history of a given lineage, which is clearly not true since most lineages will share some of their history with other taxa. Moreover, using Brownian motion to describe the adaptive process is inherently inappropriate (Hansen 1997; Butler and King 2004; Hansen and Orzack 2005; Hansen et al. 2008; Hansen 2014) and could lead to type I errors.

However, the statistical properties of OU models have been less explored than for other methods, and this could lead to errors in model choice and parameter estimation (Boettiger et al. 2012; Ho and Ané 2014; Cressler et al. 2015; Cooper et al. 2016). Cooper et al. (2016) showed that comparing single-optimum OU models to Brownian motion with a likelihood ratio test (LRT) produced high type I error rates and suggested using phylogenies with at least 200 species for such comparisons. However, Cooper et al. (2016) did not examine more complex multiple-regime OU models, as I do in this article, so it is unclear how their results translate to the model comparisons herein. More relevant to my analyses, Cressler et al. (2015) examined the statistical properties of OU models with multiple selective regimes. In particular, they found that model selection was often highly accurate, even under conditions when parameter estimation was poor. For example, model selection could be highly accurate when simulating three selective regimes on a 30-species phylogeny. This suggests that my current approach is appropriate, given that the optimal models for my 44-species tree had either a single OU regime (jumping performance) or two regimes (swimming performance). Moreover, the six-regime models favored for morphology in the current article were fit on a 191-species phylogeny, which should be powerful enough to discriminate competing models.

Nonetheless, I examined the power of my data to discriminate among models by using the parametric bootstrapping simulations recommended by Boettiger et al. (2012). In addition, I used this same simulation approach to compare models to avoid committing type I errors (i.e., when using AICc model selection alone). I note, however, that such simulations are geared toward hypothesis testing among models, not comparing the strength of different models in an information-theoretic framework, as I do in this article. Regardless, both AICc model selection and parametric bootstrapping gave similar results (see below).

Parametric bootstrapping simulations can be used to compare two models at a time. For example, one might wish to see whether the data favor rejecting a simple model (e.g., single-optimum OU) in favor of a more complex model (e.g., six-optimum microhabitat OU). Thus, for a given model comparison I first simulated 500 new data sets under both the simple and the more complex model (for 1,000 data sets total) using the maximum likelihood parameters estimated from my data for each model. I next calculated the likelihood of both models on both sets of simulated data to calculate (1) P values for model comparison and (2) the power of my data to discriminate models. First, for each

simulation replicate I estimated the likelihood of both the simple and the more complex model for the simple-simulated data and calculated a LRT. The distribution of these LRT statistics represents a null distribution for hypothesis testing. Thus, to calculate a *P* value I compared the empirical LRT value (from my data) to the distribution of LRT values obtained by simulation under the simpler model. Second, I estimated the likelihood of both the simple and the more complex model for the complex-simulated data and calculated their LRT statistics. The proportion of these LRT statistics that is greater than the LRT statistic that defines the 5% right tail of the null distribution (as produced in the previous step) gives the power of the model comparison. Generally but not always, a test with low power will also have high type I error rates with the standard LRTs (Boettiger et al. 2012).

Here I compared multiple models for each of the six phenotypic variables (RLL and RLMM, jumping velocity and acceleration, and swimming velocity and acceleration) separately and also as two-variable multivariate models, as in the main methods, for a total of nine sets of simulations. In the case of morphology and jumping performance, I simulated data under three models: Brownian motion, single-optimum OU, and microhabitat-specific OU. For swimming performance, I also simulated data for the swimming ecomorph model (i.e., whether adults regularly swim outside the breeding season), given that this was the favored model under AICc model selection for both swimming velocity and acceleration. All parametric bootstrapping analyses were done with the R packages pmc (ver. 1.0.2; Boettiger et al. 2012) and ouch (ver. 2.9-2; Butler and King 2004; King and Butler 2009). Note that one typically compares nested models with LRTs (e.g., when comparing the LRT statistic to a χ^2 distribution) and that the Brownian motion model is not nested within the OU models in ouch (O'Meara and Beaulieu 2014). Moreover, OU models in general are often nonnested due to heterogeneous regime mapping on internal branches (Boettiger et al. 2012). However, models do not need to be nested in this approach, as the LRT statistic is simply a metric to compare models (i.e., one would obtain similar results using other model comparison metrics).

The parametric bootstrapping simulations were almost universally concordant with AICc-based model selection and often showed very high power to distinguish models. For the 191-species tests of morphology, parametric bootstrapping simulations favored the microhabitat model over the single-optimum OU model (RLL: $P = .006$; RLMM: $P = .000$; multivariate: $P = .000$; fig. A5), the same results as AICc model comparison, and these analyses had high statistical power (RLL = 0.968; RLMM = 0.996; multivariate = 1.000).

As in AICc model selection, the single-optimum model was also favored in parametric bootstrapping simulations of jumping velocity evolution; these analyses supported rejecting Brownian motion ($P = .006$) and not rejecting the single-optimum model in favor of the microhabitat model ($P = .128$). The data showed reasonably high power to distinguish models (Brownian motion vs. OU1 = 0.884, OU1 vs. microhabitat = 0.634; fig. A6). For jumping acceleration, simulations slightly supported Brownian motion over a single-optimum OU model (Brownian motion vs. OU1: $P = .154$; OU1 vs. microhabitat: $P = .970$), although statistical power to distinguish models was very low (Brownian motion vs. OU1 = 0.168; OU1 vs. microhabitat = 0.060). Finally, simulations favored the single-optimum OU model for the multivariate evolution of jumping performance (i.e., velocity and acceleration together; Brownian motion vs. OU1: $P = .012$, power = 1.000; OU1 vs. microhabitat: $P = .256$, power = 0.616).

Simulations also favored similar models as AICc model selection in the evolution of swimming performance, and comparisons were statistically powerful in most cases (fig. A7). The single-optimum OU model was rejected in favor of the swimming ecomorph model (velocity: $P = .008$, power = 0.890; acceleration: $P = .010$, power = 0.728; multivariate: $P = .002$, power = 0.890), while the microhabitat model was not favored over the swimming ecomorph model (velocity: $P = .066$, power = 0.772; acceleration: $P = .684$, power = 0.242; multivariate: $P = .160$, power = 0.718).

Finally, I also used parameter variation across bootstrapping replicates of the optimal model for each trait to calculate 95% confidence intervals of the OU parameters, which will further allow distinction of ecomorphs. For example, if these intervals show that a leg-morphology adaptive optimum of one type of ecomorph is significantly different from that of another but performance model comparison shows that these same ecomorphs have similar jumping performance optima, then this would be evidence of many-to-one mapping of morphology onto performance.

Testing the Power and Potential Inaccuracy of Multivariate Model Comparison

In this article I mostly examine univariate relationships, but I also consider two-trait multivariate models to characterize the evolution of overall leg morphology, jumping performance, and swimming performance. I also expected such multivariate models to have higher statistical power to discriminate different evolutionary scenarios (Manly 1994;

Zar 1999). To determine whether these models are actually more powerful in the current analysis, I first estimated power using the phylogenetic Markov chain Monte Carlo simulation method of Boettiger et al. (2012), as described above. These simulations showed that the power to discriminate models of evolution was often higher than in univariate tests (table A8). In morphology, the multivariate model showed higher power than either univariate analysis (i.e., RLL or RLMM alone). For jumping performance, the multivariate model showed higher power to reject Brownian motion in favor of the single-optimum OU model (the one favored by AICc), although the multivariate analysis was slightly weaker than analyzing velocity alone when comparing the single-optimum and microhabitat-based OU models. Results for swimming performance were similar to those of jumping performance (table A8).

Despite this potential advantage of multivariate models, Adams and Collyer (2018) showed that model choice can frequently be inaccurate (i.e., the correct model is misspecified) when comparing multivariate models of phenotypic evolution with many traits. The exact model misspecification rate depends on the method used, the exact implementation of that method (e.g., the R package), the number of traits, and sometimes the covariation between traits (Adams and Collyer 2018). They found lowest error rates when using LRTs or AIC to compare multivariate likelihood models with the lowest number of traits.

Adams and Collyer (2018) only examined results for four or more trait dimensions when considering OU models, so it is unclear how their results apply to the minimum multivariate case of two traits that I examine here. Thus, I estimated model misspecification rates for two traits by conducting simulations using a minor modification of Adams and Collyer's (2018) simulation code, posted as part of their supplemental material (https://doi.org/10.5061/dryad.29722). I simulated Brownian motion evolution for two traits (with no covariation, as it is arbitrary; Adams and Collyer 2018) along 500 random splits-generated phylogenies of 32 species. I then estimated the likelihood of both Brownian motion and a single-optimum OU model in ouch (Butler and King 2004; King and Butler 2009), the R package I used for my main analyses. Finally, I compared models using AICc and considered the more complex model to be supported when its AICc was at least 4.0 units lower than that of the simulated Brownian motion model (as in Adams and Collyer 2018). By this criterion, I found model misspecification in only 4.8% of the simulations, an acceptable level compared with the nominal 5% type I error rate of most statistical tests.

Additional Tests of the Importance of Relative Leg Length versus Muscle Mass in Swimming Performance

The morphological tests showed that ecomorphs that regularly swim (e.g., aquatic) have higher RLMM than other ecomorphs, and I found the same pattern in swimming velocity (see "Results"). Thus, a key goal of these regression analyses was to test whether the fit between robust muscular legs and high swimming velocity in swimming ecomorphs results from leg muscle mass being more important than leg length for swimming performance. The most direct evidence would be finding that only leg muscle mass (and not leg length) was in the optimal regression model of swimming velocity. However, both variables were in the optimal model (see "Results"). Thus, I addressed the importance of leg muscle mass on swimming velocity in three other ways. Given the similarity of results across the three methods, I present the first two here and the third in the main text.

First, I compared the summed AICc weight of RLL and that of RLMM across all models for both jumping and swimming velocity. AICc weights allow one to examine the statistical support for a single variable across all models regardless of the support for any single model. For example, if a variable is found in all models that have some AICc weight, then regardless of the ability of the data to support a specific whole model, one can say that the data do support the importance of that single variable across models (Burnham and Anderson 2002; Johnson and Omland 2004; Posada and Buckley 2004). Here I compared the total summed AICc weights of the two leg predictor variables and asked whether one had a higher weight than the other across all models of jumping and swimming velocity. I predicted that leg muscle mass would have a higher weight than leg length in swimming velocity but not necessarily in jumping velocity. However, these summed weights for RLL and RLMM were similar for peak jumping velocity (RLL: $\Sigma w_i = 0.998$; RLMM: $\Sigma w_i = 0.992$) and swimming velocity (RLL: $\Sigma w_i = 0.997$; RLMM: $\Sigma w_i = 0.998$).

Second, I compared the amount of independent variation explained by RLMM and RLL in jumping and swimming velocity. Because both leg variables are important parts of the optimal models of jumping and swimming velocity and because they are correlated (PGLS in the 44 species with performance data: $r = 0.683$), I wanted to examine how much variation in the response variables each leg predictor variable explained alone. To do this, I started with the optimal model for each response variable, which had both of these leg predictor variables (see "Results"). Then

I subtracted each leg predictor variable from that optimal model and examined the drop in adjusted R^2. This drop represents the variation that the removed leg predictor variable explains alone; a higher drop in variation thus represents a higher importance of a given leg predictor variable in explaining variation in the response variable. For example, microhabitat, RLL, and RLMM were the predictor variables in the optimal model for peak swimming velocity. Thus, when I subtract the R^2 of a model with just microhabitat and RLMM from the R^2 of the full model, I am calculating the additional variation explained by RLL alone in the full model. Doing this for both leg predictor variables allowed me to compare the variation explained by each alone in both jumping and swimming velocity. These changes in R^2 when sequentially removing variables suggested that both variables explained similar independent variation in swimming velocity (RLL: $\Delta R^2 = 0.098$; RLMM: $\Delta R^2 = 0.109$) and jumping velocity (RLL: $\Delta R^2 = 0.145$; RLMM: $\Delta R^2 = 0.137$).

Finally, I calculated and compared standard partial regression coefficients to measure the relative impact of variation in RLL and RLMM on variation in jumping and swimming velocity. Such coefficients can be used to compare the relative importance of variables in multiple regression (Sokal and Rohlf 1995) and have been suggested specifically in the case of studying multivariate character evolution and trade-offs (Ghalambor et al. 2003; Walker 2007). Standard partial regression coefficients are simply the regression coefficients obtained when first standardizing predictor variables to unit mean and variance (Sokal and Rohlf 1995), which puts all variables on a common scale of variation. In other words, with these coefficients I was able to compare how the response variable (jumping or swimming velocity) changed with respect to a 1 standard deviation of change in each predictor variable (RLL or RLMM). For example, to examine whether RLMM had a larger influence than RLL on swimming velocity, I calculated standard partial regression coefficients and compared the values. A larger importance of RLMM would be shown by having a higher coefficient than RLL—that is, if the former were more influential, a 1 standard deviation change in it would lead to more change in swimming velocity than a 1 standard deviation change in RLL.

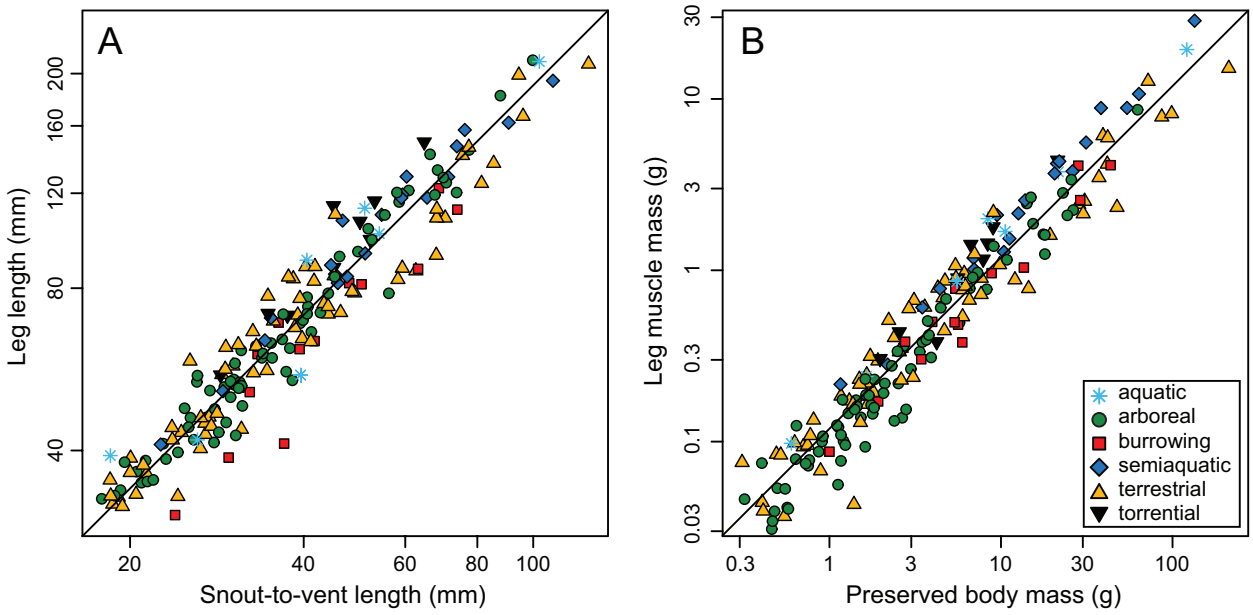

Figure A1: Regressions of leg length (*A*) and preserved leg muscle mass (*B*) on body length (snout-to-vent length; *A*) and preserved body mass (*B*) for the 191-species morphology data set (the 44-species morphology-performance data set was a subset of the 191-species data set). All plots show variables in original units on a log scale, and lines indicate isometric lines (slope of 1.0), which nearly always fell within the 95% confidence intervals of best-fit lines (table A1). Color and symbol legend applies to both panels.

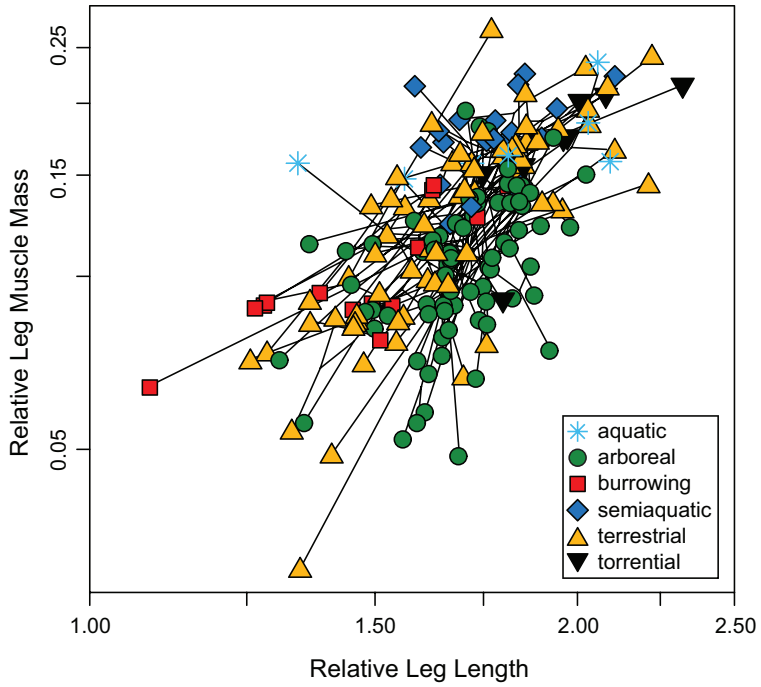

Figure A2: Phylomorphospace of anuran leg morphology. All aspects are as in figure 3, with the addition of the phylogeny linking species in this figure. The phylogeny shows the extreme convergence in morphology across species (see also Moen et al. 2016), thus emphasizing that common ancestry is often insufficient (at least in this sample of species) to explain the realized morphology of species.

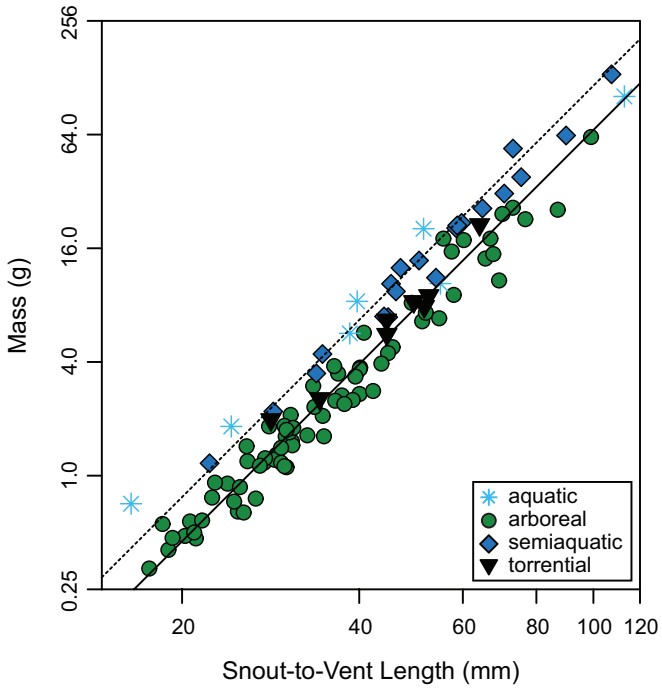

Figure A3: Regression of body mass (g) on snout-to-vent length (mm) and ecomorph type. The dotted line is the regression line for aquatic and semiaquatic species together (light blue asterisks and dark blue diamonds, respectively), while the solid line is for arboreal species (green circles). The lines differ only in intercept, not slope ($b = 3.11$), indicating that aquatic and semiaquatic species have more mass than arboreal species for their body length. Torrential species (black upside-down triangles) are shown for additional illustration. Note that the vertical axis is compressed to 33% of the isometric height. Both variables are shown in original units on a log scale.

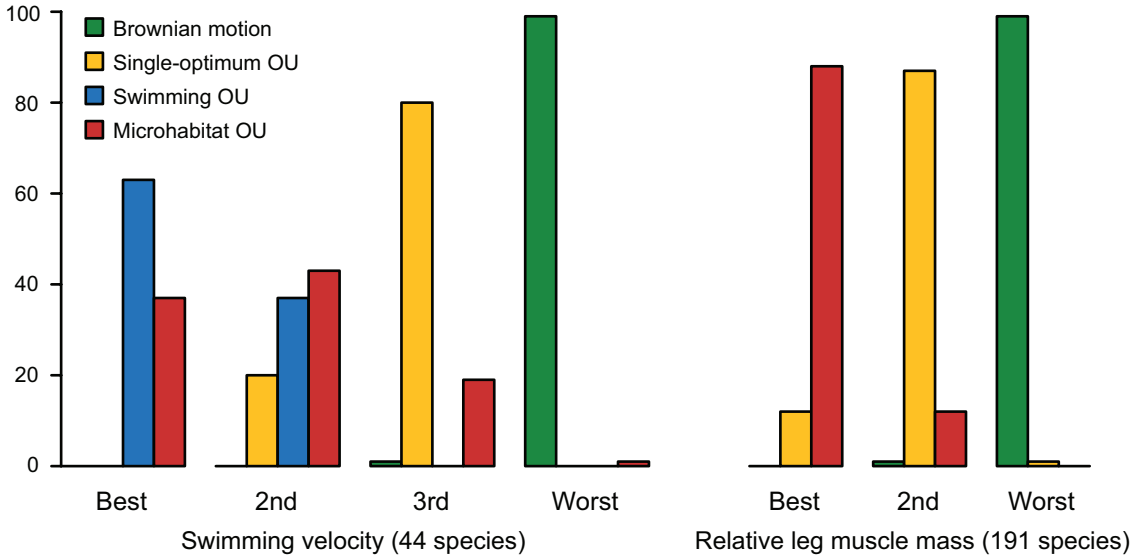

Figure A4: Histograms showing ranks of models across stochastic mapping replicates. For each of 100 replicates, models were ranked on the basis of their corrected Akaike information criterion (AICc). Histograms show the number of ranks for each model across those replicates. For both relative leg muscle mass (191 species) and swimming velocity (44 species), the most frequently top-ranked model corresponds to the model favored in the primary analyses (i.e., Ornstein-Uhlenbeck [OU] model fitting with likelihood-estimated ancestral state estimates). The frequency of being ranked first also roughly corresponded to mean AICc weight across replicates (table A7).

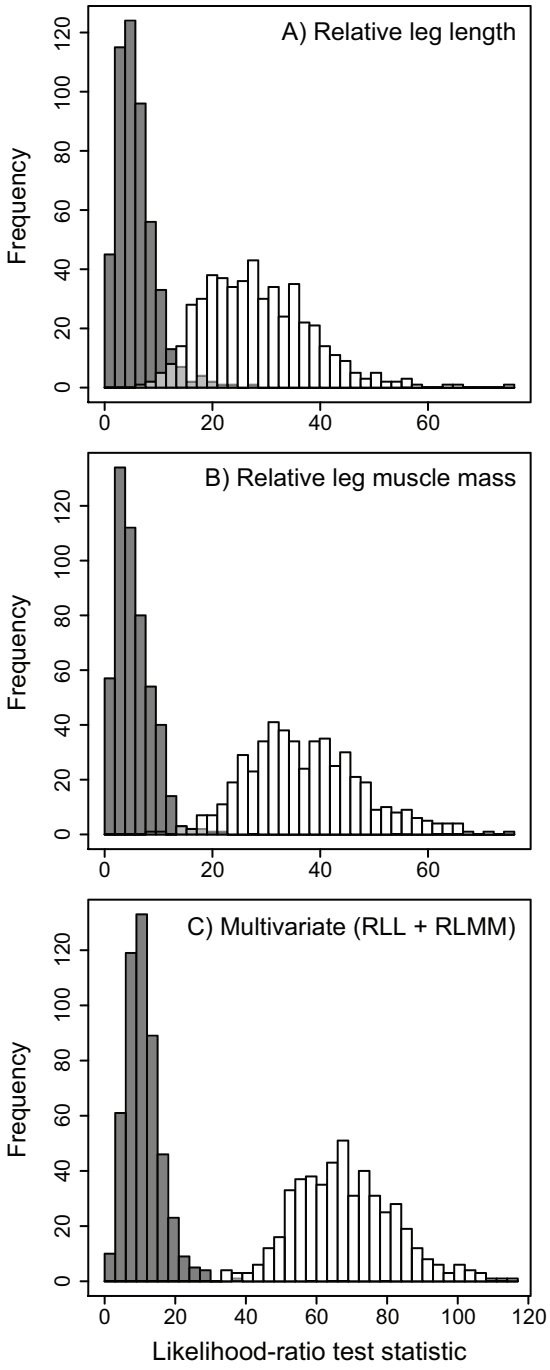

Figure A5: Histograms of parametric bootstrapping results for comparing a single-optimum Ornstein-Uhlenbeck (OU) model and an ecomorph-based OU model of morphological evolution across 191 species. Dark gray bars represent likelihood ratio test (LRT) statistics when both models are fit to data simulated under the simpler model, whereas white bars are the LRT statistics when both models were fit to data simulated under the more complex model. Light gray represents overlap in distributions, with the light gray portion indicating whichever bar is shorter in that section. RLL = relative leg length; RLMM = relative leg muscle mass.

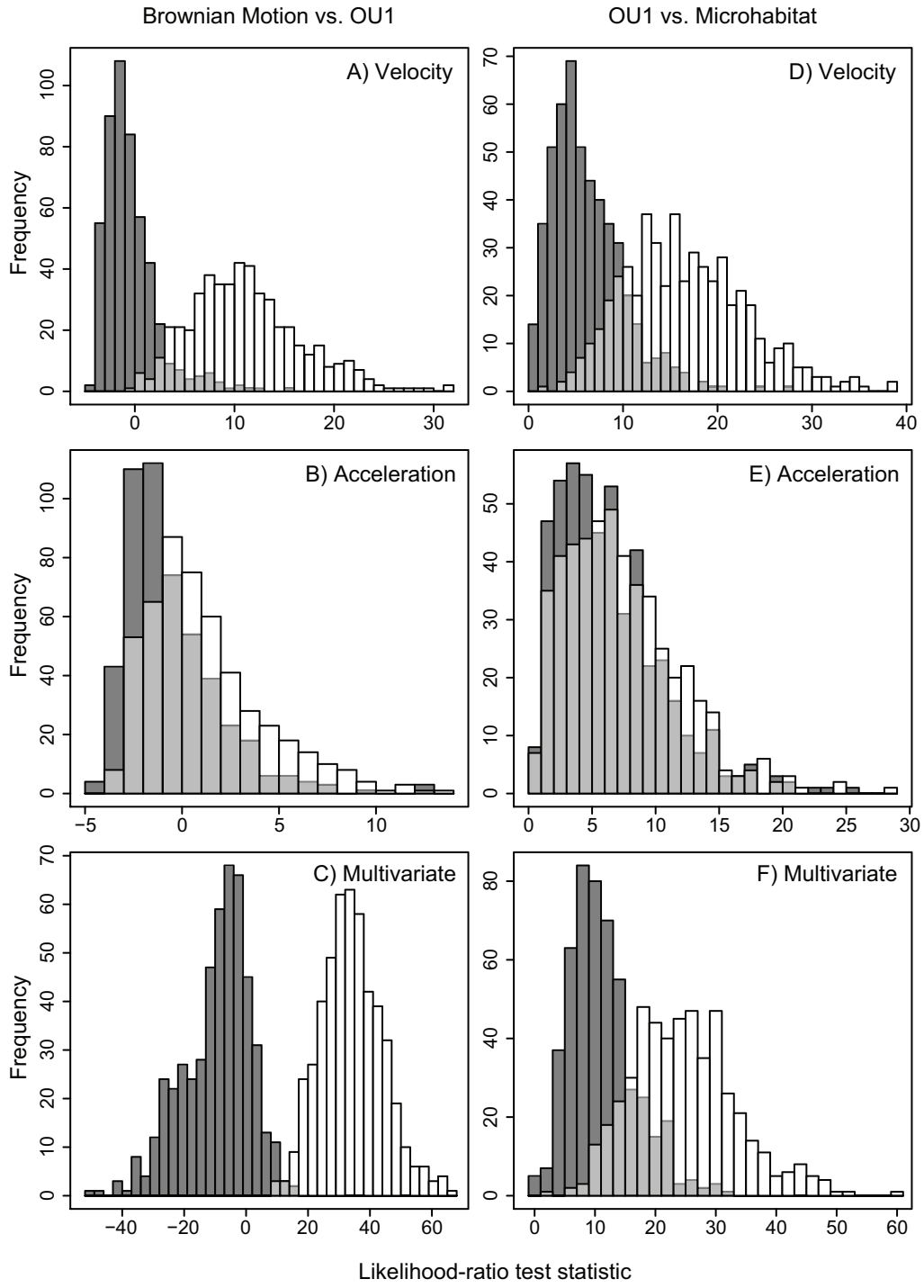

Figure A6: Histograms of parametric bootstrapping results for comparing Ornstein-Uhlenbeck (OU) models of the evolution of jumping performance across 44 species. Bar colors are the same as in figure A5. Multivariate models in *C* and *F* represent models of joint evolution in jumping velocity and acceleration. Titles above each column (*A–C*, *D–F*) represent which model comparison the histograms represent, with the simpler model indicated at left.

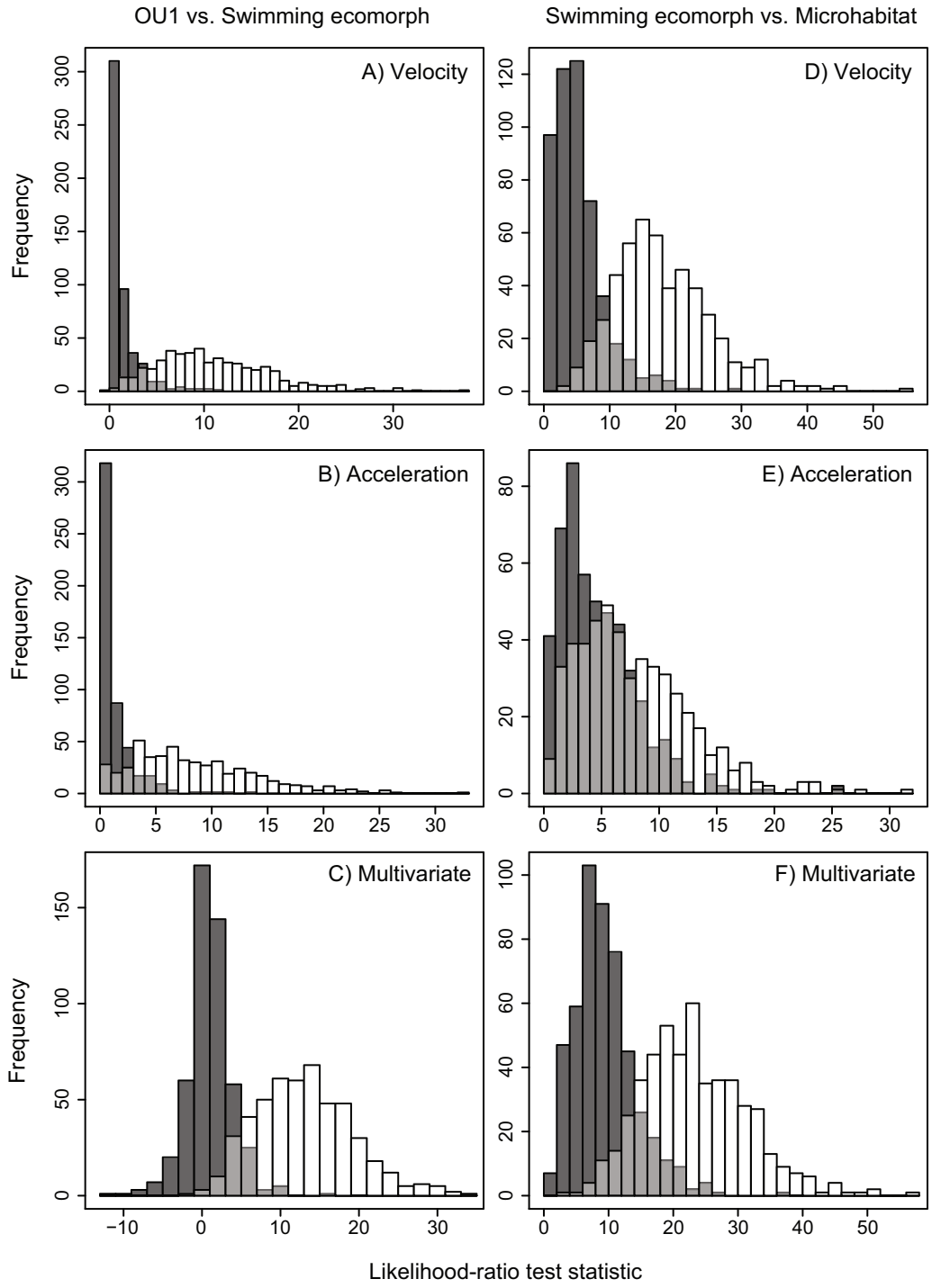

Figure A7: Histograms of parametric bootstrapping results for comparing Ornstein-Uhlenbeck (OU) models of the evolution of swimming performance across 44 species. Bar colors are the same as in figure A5. Multivariate models in *C* and *F* represent models of joint evolution in swimming velocity and acceleration. Titles above each column (*A–C*, *D–F*) represent which model comparison the histograms represent, with the simpler model indicated at left.

Table A1: Results of scaling analyses between leg variables (leg length, preserved leg muscle mass) and standardizing size variables (body length [snout-to-vent length], preserved body mass)

Data set, focal variable, size variable	Regression type	MLE of slope (95% CI)
Morphology only (191 species):		
Leg length, body length	Standard	.966 (.926–1.005)
Leg length, body length	PGLS	.986 (.950–1.021)
Leg muscle mass, body mass	Standard	1.028 (.991–1.065)
Leg muscle mass, body mass	PGLS	1.037 (1.002–1.072)
Morphology and performance (44 species):		
Leg length, body length	Standard	1.017 (.934–1.101)
Leg length, body length	PGLS	1.044 (.962–1.127)
Leg muscle mass, body mass	Standard	1.052 (.975–1.129)
Leg muscle mass, body mass	PGLS	1.074 (.998–1.151)

Note: All analyses were done on logged variables; thus, a slope of 1.0 indicates an isometric relationship between variables. Phylogenetic generalized least squares (PGLS) analyses allowed λ (the phylogenetic scaling parameter) to take its maximum likelihood value (Revell 2010); these were all high (e.g., all $\lambda > 0.855$). CI = confidence interval; MLE = maximum likelihood estimate.

Table A2: Breeding habitat data (i.e., breed in water or not) for species with swimming performance data

Species	Breed in water	Source
Adenomera hylaedactyla	No	AmphibiaWeb 2016
Allobates femoralis	No	AmphibiaWeb 2016
Ameerega trivittata	No	AmphibiaWeb 2016
Amolops tuberodepressus	Yes	IUCN 2014
Babina pleuraden	Yes	IUCN 2014
Chiasmocleis bassleri	Yes	IUCN 2014
Chiromantis doriae	Yes	IUCN 2014
Cyclorana australis	Yes	AmphibiaWeb 2016
Cyclorana longipes	Yes	AmphibiaWeb 2016
Dendropsophus rhodopeplus	Yes	IUCN 2014
Dendropsophus sarayacuensis	No	AmphibiaWeb 2016
Dendropsophus triangulum	No	IUCN 2014
Duttaphrynus melanostictus	Yes	AmphibiaWeb 2016
Glyphoglossus yunnanensis	Yes	IUCN 2014
Hamptophryne boliviana	Yes	IUCN 2014
Hyla annectans	Yes	IUCN 2014
Hypsiboas hobbsi	Yes	IUCN 2014
Hypsiboas lanciformis	Yes	IUCN 2014
Hypsiboas punctatus	Yes	IUCN 2014
Leptodactylus leptodactyloides	Yes	IUCN 2014
Leptodactylus rhodomystax	Yes	IUCN 2014
Limnodynastes convexiusculus	Yes	AmphibiaWeb 2016
Litoria bicolor	Yes	AmphibiaWeb 2016
Litoria caerulea	Yes	AmphibiaWeb 2016
Litoria dahlii	Yes	AmphibiaWeb 2016
Litoria inermis	Yes	AmphibiaWeb 2016
Litoria nasuta	Yes	AmphibiaWeb 2016
Litoria pallida	Yes	AmphibiaWeb 2016
Litoria rothii	Yes	AmphibiaWeb 2016
Litoria rubella	Yes	AmphibiaWeb 2016
Litoria tornieri	Yes	AmphibiaWeb 2016
Microhyla fissipes	Yes	IUCN 2014
Nanorana yunnanensis	Yes	AmphibiaWeb 2016
Odorrana grahami	Yes	IUCN 2014
Oreobates quixensis	No	IUCN 2014
Osteocephalus planiceps	No	IUCN 2014

Table A2 (*Continued*)

Species	Breed in water	Source
Platyplectrum ornatum	Yes	AmphibiaWeb 2016
Rhacophorus dugritei	Yes	IUCN 2014
Rhacophorus rhodopus	Yes	IUCN 2014
Rhinella margaritifera	Yes	IUCN 2014
Rhinella proboscidea	Yes	AmphibiaWeb 2016
Scinax ruber	Yes	AmphibiaWeb 2016
Sphaenorhynchus lacteus	Yes	AmphibiaWeb 2016
Uperoleia lithomoda	Yes	AmphibiaWeb 2016

Table A3: Morphological parameter estimates from the microhabitat-based Ornstein-Uhlenbeck (OU) model of evolution (the optimal model chosen by corrected Akaike information criterion, following table 1)

Parameter	Relative leg length (95% CI)	Relative leg muscle mass (95% CI)
α	1.316 (.746–3.280)	3.651 (2.496–7.755)
σ^2	.044 (.034–.071)	.733 (.521–1.296)
Aquatic θ	1.572 (1.235–2.089)	.190 (.130–.290)
Arboreal θ	1.531 (1.343–1.770)	.096 (.080–.116)
Burrowing θ	1.087 (.798–1.412)	.086 (.064–.114)
Semiaquatic θ	1.615 (1.323–1.901)	.176 (.136–.226)
Terrestrial θ	1.621 (1.460–1.801)	.128 (.114–.144)
Torrential θ	2.283 (1.671–3.260)	.164 (.114–.234)

Note: Numbers are maximum likelihood parameter estimates followed by 95% confidence intervals (CIs) estimated by 500 parametric bootstrapping simulation replicates. α = rate of movement toward an evolutionary optimum; σ^2 = rate of Brownian motion evolution; θ = evolutionary optimum of an OU model. When interpreting values of α and σ^2, note that the R package ouch scales the phylogeny to a length of 1.0. The θ have no units here, as they are relative values (i.e., relative to body length and body mass). Raw values of ratios are shown here, but logged ratios were analyzed.

Table A4: Parameter estimates of the microhabitat Ornstein-Uhlenbeck (OU) model of relative leg muscle mass (RLMM) evolution when leg muscle mass was standardized by leg length (instead of body mass, as in most analyses)

Parameter	RLMM (95% CI)
α	10.25 (6.57–26.58)
σ^2	6.23 (4.17–17.47)
Aquatic θ	.0185 (.0066–.0453)
Arboreal θ	.0037 (.0027–.0049)
Burrowing θ	.0117 (.0063–.0211)
Semiaquatic θ	.0280 (.0164–.0490)
Terrestrial θ	.0069 (.0053–.0091)
Torrential θ	.0104 (.0053–.0228)

Note: Numbers are maximum likelihood parameter estimates followed by 95% confidence intervals (CIs) estimated by 500 parametric bootstrapping simulation replicates. α = rate of movement toward an evolutionary optimum; σ^2 = rate of Brownian motion evolution; θ = evolutionary optimum of leg length–standardized leg muscle mass for a given ecomorph. When interpreting values of α and σ^2, note that the R package ouch scales the phylogeny to a length of 1.0. The θ have units of grams of muscle mass per millimeter of leg length. Raw values of ratios are shown here, but logged ratios were analyzed. The microhabitat OU model was strongly favored (corrected Akaike information criterion [AICc] = 511.0) over single-optimum OU (AICc = 540.0) and Brownian motion (AICc = 561.3) models.

Table A5: Parameter estimates from the optimal evolutionary models of performance variables

Variable, model	Velocity (95% CI)	Acceleration (95% CI)
Jumping:		
Optimal model	Single-optimum OU	Brownian motion
α	3.640 (1.782–179.7)	...
σ^2	2.461 (1.142–103.647)	1,738.8 (1,050.9–2,429.0)
Single θ	2.322 (2.093–2.560)	...
Swimming:		
Optimal model	Swim regularly	Swim regularly
α	3.234 (1.510–41.638)	2.826 (1.430–40.948)
σ^2	.706 (.348–6.545)	483.7 (237.0–5024.9)
No swim θ	.962 (.785–1.113)	26.639 (21.708–31.288)
Swim θ	1.744 (1.270–2.391)	46.070 (30.757–65.044)

Note: Optimal models were chosen with the corrected Akaike information criterion (AICc) following table 2; see the main text for model descriptions. Numbers are maximum likelihood parameter estimates followed by 95% confidence intervals (CIs) estimated by 500 parametric bootstrapping simulation replicates. α = rate of movement toward an evolutionary optimum; σ^2 = rate of Brownian motion evolution; θ = evolutionary optimum of an Ornstein-Uhlenbeck model. θ is in units of meters per second (m/s) for velocity and meters per second squared (m/s^2) for acceleration. When interpreting values of α and σ^2, note that the R package ouch scales the phylogeny to a length of 1.0. Moreover, note that the rate of evolution (σ^2) is so much larger in acceleration than velocity because values of acceleration were one to two orders of magnitude higher than velocity (i.e., the rate of evolution will reflect a variance that is two to four orders of magnitude higher).

Table A6: Reevaluating the optimal model of jumping performance evolution in light of results for swimming performance

Variable, model	K	$\ln L$	AICc	ΔAICc	w_i
Jumping velocity:					
Brownian motion	2	−41.88	88.05	8.79	.007
OU single optimum	**3**	**−36.33**	**79.26**	**.00**	**.543**
Swim regularly	4	−35.42	79.87	.61	.400
Microhabitat	8	−31.96	84.03	4.77	.050
Jumping acceleration:					
Brownian motion	**2**	**−205.89**	**416.08**	**.00**	**.523**
OU single optimum	3	−205.14	416.88	.80	.351
Swim regularly	4	−204.96	418.95	2.87	.125
Microhabitat	8	−204.20	428.51	12.43	.001

Note: Results for both jumping velocity and acceleration are similar including the "swim regularly" model as with the original three models, except that the former shows reasonable support for jumping velocity. Methods and interpretation of this table are the same as table 2. K is the number of parameters in each model. $\ln L$ is their log likelihood. AICc is the corrected Akaike information criterion. ΔAICc is the difference between a given model and the optimal model for a performance variable (that with the lowest AICc, shown in boldface). w_i are the AICc weights of models. OU = Ornstein-Uhlenbeck.

Table A7: Comparing the strength of Ornstein-Uhlenbeck (OU) models when using Bayesian stochastic character mapping to estimate internal states

Variable, model	K	simmap w_i	Main w_i
Relative leg muscle mass (191 species):			
Brownian motion	2	.003 ± .0003	.000
OU single optimum	3	.198 ± .0193	.000
Microhabitat	**8**	**.799 ± .0196**	**1.000**
Swimming velocity (44 species):			
Brownian motion	2	.004 ± .0003	.001
OU single optimum	3	.049 ± .0030	.015
Swim regularly	**4**	**.569 ± .0289**	**.559**
Microhabitat	8	.378 ± .0311	.420

Note: K is the number of parameters in each model. simmap w_i shows the mean and standard error of corrected Akaike information criterion (AICc) weights of models across all 100 simulated stochastic maps. Main w_i is the AICc weight for a model as found with the primary analyses (i.e., using likelihood-estimated internal states; from tables 1 and 2). Boldfacing indicates the most highly supported model for each response variable.

Table A8: Comparing the power of two-variable multivariate analyses to distinguish evolutionary models and the power of their underlying single variables when analyzed alone

	Power	
Model, response variable(s)	Comparison 1	Comparison 2
Morphology (191 species):		
Relative leg length	.398	.968
Relative leg muscle mass	.920	.996
Both (multivariate)	.984	1.000
Jumping performance (44 species):		
Velocity	.884	.634
Acceleration	.168	.060
Both (multivariate)	1.000	.616
Swimming performance (44 species):		
Velocity	.890	.772
Acceleration	.728	.242
Both (multivariate)	.890	.718

Note: Comparison 1 tested the power to either reject Brownian motion in favor of a single-optimum Ornstein-Uhlenbeck (OU) model (morphology, jumping performance) or reject a single-optimum OU model in favor of the swimming ecomorph model (swimming performance). Comparison 2 tested the power to reject a single-optimum OU model (morphology, jumping performance) or the swimming ecomorph model (swimming performance) in favor of the microhabitat model. Statistical power was estimated with parametric bootstrapping, in which trait evolution was simulated under the more complex model using maximum likelihood parameters estimated from the empirical data. Power was simply the frequency of simulation replicates (500) in which the simpler (incorrect) model was rejected in favor of the more complex (simulated) model.

 DOI: 10.1086/704736

Appendix B from D. S. Moen, "What Determines the Distinct Morphology of Species with a Particular Ecology? The Roles of Many-to-One Mapping and Trade-Offs in the Evolution of Frog Ecomorphology and Performance" (Am. Nat., vol. 194, no. 4, p. E000)

Museum Specimens Used in This Study

Table B1: Museum numbers of all specimens used in this study

Species	Museum nos.
Acris crepitans	USNM435236, 435237, 435242, 435244, 435258
Acris gryllus	USNM526326, 526330, 526372, 526380, 526386
Adenomera andreae	USNM222256, 222257, 222259−222261
Adenomera hylaedactyla	DSM0131, 0177, 0178, 0180, 0186
Afrixalus laevis	CAS202032, 202033, 202035, 202106, 202108
Aglyptodactylus madagascariensis	MCZ.A-119870, 119872, 119888, 119892, 119895
Allobates femoralis	DSM0113
Ameerega picta	USNM247114, 268838, 268839, 268840, 342507
Ameerega trivittata	DSM0128, 0129
Amietia angolensis	CAS177181, 177182, 177191, 202040
Amnirana albolabris	CAS177137, 177138, 177139, 202204
Amolops tuberodepressus	KIZ04113, 04155, 04158, 04178, 04202
Anaxyrus americanus	USNM528746, 528748, 528750, 528752, 528756
Anaxyrus fowleri	USNM528968−528972
Ansonia leptopus	FMNH138821, 138833, 194730, 194748, 195108
Aplastodiscus arildae	USNM208735, 247814, 247815, 303021
Arthroleptis schubotzi	CAS201717, 201719, 201737, 201738, 201739
Babina pleuraden	KIZ04140, 04144, 04159, 04167, 04182, 04183
Blommersia blommersae	MCZ.A-136667, 136670
Bokermannohyla circumdata	USNM208745, 208752, 208755, 208756, 208783
Bokermannohyla hylax	USNM129107, 208777, 208780, 247811, 247812
Boophis cf. *miniatus*	MCZ.A-120340, 120547, 120576, 120660, 120664
Boophis madagascariensis	MCZ.A-119958, 119965, 120143
Boophis reticulatus	MCZ.A-120389, 120391, 120623
Breviceps adspersus	CAS200128, 200129, 200131
Bufo spinosus (as *B. bufo*)	CM54215, 54705, 54705B, 55750
Ceratophrys cornuta	USNM222264, 342848, 343238
Chiasmocleis bassleri	DSM0109−0112, 0130
Chiromantis doriae	KIZ04136, 04146, 04148, 04171
Craugastor brocchi	KU186150, 186156, 189621, 189634, 189640
Craugastor lineatus	KU186165, 186172, 186181, 186184, 189670
Crossodactylus dispar	USNM318198, 318199, 318200, 318201, 318227
Cyclorana australis	DSM0207−210, 0237, 0292
Cyclorana longipes	DSM0238, 0239, 0256, 0279−0281
Dendropsophus microps	USNM243572, 243573, 243574, 243575, 247826
Dendropsophus minutus	USNM208841, 208842, 208847, 303042, 303043
Dendropsophus parviceps	USNM247171, 247173, 247174, 247180, 247599
Dendropsophus rhodopeplus	USNM342946, 342947, 342948, 342949, 345247; DSM0045
Dendropsophus sarayacuensis	USNM342955, 342956, 342957, 342958, 343214; DSM0046, 0132, 0134, 0135, 0137, 0138, 0140
Dendropsophus triangulum	DSM0055, 0056, 0059, 0060, 0062, 0063, 0066
Discoglossus jeanneae	CM52477, 52509, 52513, 52538, 52553
Duttaphrynus melanostictus	KIZ04112, 04154, 04173, 04179, 04188
Duttaphrynus parietalis	FMNH218187, 218188, 218189, 218193, 218195, 218196, 218197

Table B1 (*Continued*)

Species	Museum nos.
Elachistocleis ovalis (as *E. bicolor*)	USNM247434, 343271, 343272, 343273
Engystomops petersi	USNM222307, 247426, 247659, 343260, 343265
Epidalea calamita	CM54316, 54316B, 54316D, 54316E, 54634C
Fejervarya keralensis	FMNH217986, 217987, 217988, 217990, 217993
Fritziana ohausi	USNM217714, 217715, 217716, 217720, 217721
Gastrophryne carolinensis	USNM529690, 529692, 529694, 529696, 529698
Gephyromantis asper	MCZ.A-120644, 120738
Gephyromantis luteus	MCZ.A-119983, 119995, 119998, 120000, 120002
Glyphoglossus smithi	FMNH136321, 244685
Glyphoglossus yunnanensis	KIZ04197
Guibemantis depressiceps	MCZ.A-120584, 120737
Guibemantis liber	MCZ.A-120040, 120044, 120052, 120059, 136287
Guibemantis pulcher	MCZ.A-120763
Haddadus binotatus	USNM209124, 209127, 209132, 209133, 209137
Hamptophryne boliviana	USNM247438, 247661, 247665, 343034, 343037; DSM0188, 0189, 0190, 0191
Heterixalus alboguttatus	MCZ.A-136101, 136108, 136243
Heterixalus betsileo	MCZ.A-119911, 119913
Hyalinobatrachium fleischmanni	KU190388, 190389, 190390, 190393, 190395
Hyla annectans	KIZ04107, 04142, 04151, 04157, 04170
Hyla bocourti	KU186364, 186365, 186386, 186415, 186419
Hyla chrysoscelis	USNM530739, 530749, 530750, 530764, 530783
Hyla femoralis	USNM530867, 530868, 530870, 530874, 530969
Hyla meridionalis	CM50928, 50930, 50935, 52122, 53079
Hylarana signata	FMNH139965, 139983, 146614, 146633, 146634
Hyperolius discodactylus (as *H. alticola*)	CAS180467, 180468, 180474, 180476, 180479
Hyperolius lateralis	CAS180163, 180168, 180169, 180170, 180173
Hyperolius viridiflavus	CAS178187, 178196, 178206, 178208, 178209
Hypopachus barberi	KU186551, 186560, 186561, 186562, 186581
Hypsiboas faber	USNM208789, 208790, 208791, 247822, 247824
Hypsiboas fasciatus	USNM247141, 247145, 247584, 247585, 247590
Hypsiboas geographicus	USNM222175, 235739, 247601, 268862, 342938
Hypsiboas hobbsi	DSM0102, 0103, 0142−0145, 0149
Hypsiboas lanciformis	DSM0087, 0115, 0116, 0150−0154
Hypsiboas polytaenius	USNM208870, 208890, 208893, 208914, 208955
Hypsiboas punctatus	DSM0159, 0160, 0162−0165, 0168
Incilius ibarrai	KU186289, 186290, 186291, 186293, 186294
Indirana brachytarsus	FMNH217926, 217937, 217943, 217955, 217959
Indosylvirana temporalis	FMNH218031, 218033, 218036, 218040, 218042
Ingerophrynus divergens	FMNH138852, 138859, 138876, 138892, 138893
Ischnocnema guentheri	USNM235634, 235638, 235665, 235666, 235667
Kalophrynus pleurostigma	FMNH138068, 150432, 150433
Kaloula baleata	FMNH248861, 248862, 63499, 63500
Laliostoma labrosum	USNM149295, 149297, 499273
Leptobrachella mjobergi	FMNH138149, 138166, 138168, 138178, 146270
Leptobrachium montanum	FMNH188475, 188479, 188483, 188485
Leptodactylus bolivianus	USNM222275, 222276, 247338, 247350
Leptodactylus fuscus	USNM209217, 209218, 209219, 209220, 243685
Leptodactylus latrans	USNM209224, 209227, 209228
Leptodactylus leptodactyloides	USNM247374, 247377, 247383, 247384, 247396; DSM0051, 0169−0171, 0173, 0174, 0184
Leptodactylus petersii	USNM307120, 307122, 332459, 343255
Leptodactylus rhodomystax	DSM0052, 0053, 0067, 0101, 0105, 0107, 0123, 0124
Leptopelis kivuensis	CAS177088, 177089, 177128, 177130, 177134
Limnodynastes convexiusculus	DSM0226−0229, 0246
Limnonectes ibanorum	FMNH137233, 144213, 144290, 146879, 146908
Limnonectes kuhlii	FMNH138715, 138749, 138755, 138757
Limnonectes palavanensis	FMNH136433, 145651, 145654, 145659, 148351

Table B1 (*Continued*)

Species	Museum nos.
Litoria bicolor	DSM0266, 0268, 0271−0275
Litoria caerulea	DSM0235, 0282−0284, 0293, 0303
Litoria dahlii	DSM0230−0234, 0277, 0278, 0285
Litoria inermis	DSM0294
Litoria nasuta	DSM0212, 0214−0216, 0218−0220
Litoria pallida	DSM0222, 0276
Litoria rothii	DSM0202, 0204, 0248, 0249, 0252, 0253
Litoria rubella	DSM0194, 0197, 0198, 0201, 0247, 0254
Litoria tornieri	DSM0221, 0240, 0262, 0263, 0288, 0290, 0291, 0306
Lysapsus limellum	USNM341861, 341867, 341869, 341873, 341875
Mantella baroni	MCZ.A-120090
Mantidactylus biporus	MCZ.A-120232, 120233, 120270, 23881
Mantidactylus grandidieri	MCZ.A-136211
Mantidactylus guttulatus	MCZ.A-119984
Mantidactylus lugubris	MCZ.A-136625; USNM499327, 499328, 499499, 499502
Mantidactylus majori	MCZ.A-120026, 120070, 120071, 120182, 120183
Megophrys nasuta	FMNH139498, 139500, 145827, 145829, 148299
Meristogenys poecilus	FMNH136213, 137418, 146798, 146805, 194827
Micrixalus fuscus	FMNH218331, 218353, 218375, 218379, 218380
Microhyla fissipes	KIZ04161, 04163, 04175, 04184, 04194
Nanorana yunnanensis	KIZ04129, 04138, 04153
Nyctibatrachus major	FMNH218206, 218212, 218226, 218232, 218239
Occidozyga baluensis	FMNH157596, 157612, 157628, 196768, 196781
Odorrana grahami	KIZ04135, 04139, 04145, 04147, 04185, 04204
Odorrana hosii	FMNH139318, 139341, 144461, 144486
Oreobates cruralis	USNM342989, 342990, 342992, 343240
Oreobates quixensis	DSM0043, 0126, 0127, 0192
Osteocephalus planiceps	DSM0044, 0096, 0099, 0117, 0119, 0121
Osteocephalus taurinus	USNM222205, 247614, 342962, 342963, 342964
Pelobates cultripes	CM52103, 52105, 52106, 52643, 54584
Pelodytes ibericus	CM52109, 52110, 52111, 52115, 54702
Pelophylax perezi	CM51034, 51105, 52491, 53035, 53145
Philautus hosii	FMNH137867, 137872, 137873, 137902, 145608
Phlyctimantis verrucosus	CAS176949, 176951, 176956, 176960, 176966
Phrynobatrachus dendrobates	CAS202131, 202232, 202233, 202235, 202236
Phrynobatrachus versicolor	CAS180642, 180654, 202119, 202123, 202125
Phrynoidis aspera	FMNH137749, 137789, 137836, 144377, 144390
Phyllomedusa palliata	USNM222219, 222220, 222227, 222230, 222234
Phyllomedusa tomopterna	USNM343026, 343028, 343029, 343278, 343279
Physalaemus cuvieri	USNM243689, 243691, 243692, 243704, 243710
Physalaemus maculiventris	USNM209256, 209257, 209267, 209271, 209285
Platypelis tuberifera	MCZ.A-136201
Platyplectrum ornatum	DSM0224, 0225, 0295−0297, 0300
Plectrohyla quecchi	KU190247, 190248, 190249, 190255, 190256
Plethodontohyla notosticta	MCZ.A-136262
Polypedates macrotis	FMNH137884, 137936, 137937, 139370, 139371
Pristimantis fenestratus	USNM247304, 247631, 298796, 298875
Pristimantis reichlei	USNM247305, 247306, 268950, 268952, 268953
Proceratophrys melanopogon	USNM209306, 209310, 209313, 209314, 209315
Pseudacris brimleyi	USNM534400, 534406, 534429, 534431, 534435
Pseudacris crucifer	USNM534844, 534847, 534853, 534855, 534861
Pseudis bolbodactyla	USNM98175, 98179, 98190, 98191, 98202
Pseudis paradoxa	USNM302984, 302985, 302986, 302987, 341878
Pseudophilautus femoralis	FMNH218111, 218112, 218113, 218115, 218116
Ptychadena chrysogaster	CAS176978, 176982, 176983
Ptychadena mascareniensis	MCZ.A-120123, 120138
Ptychohyla hypomykter	KU186480, 190309, 190310, 190311, 190313
Rana berlandieri	KU186680, 190446, 190447, 190449, 190450

Table B1 (*Continued*)

Species	Museum nos.
Rana catesbeiana	USNM230366, 292158, 536602, 536604, 536618
Rana clamitans	USNM514955, 514956, 514971, 537178, 537200
Rana palustris	USNM514988, 515001, 515003, 515007, 515008
Rana sphenocephala	USNM538949, 538953, 538962, 538963, 538970
Raorchestes charius	FMNH218102, 218105, 218106, 218107
Rentapia hosii	FMNH139356, 139357, 145641, 145645, 145647
Rentapia tuberculosus	FMNH218143, 218144
Rhacophorus dugritei	KIZ04102, 04104, 04168, 04176, 04201
Rhacophorus harrissoni	FMNH137942, 137946, 137948
Rhacophorus malabaricus	FMNH217715, 217716, 217717
Rhacophorus nigropalmatus	FMNH230904, 230906, 230908, 230909, 245934
Rhacophorus pardalis	FMNH145331, 145348, 145352, 146215, 146216
Rhacophorus rhodopus	KIZ04130, 04131, 04149, 04166, 04181, 04186
Rhinella ictterica	USNM207679, 208695, 208700
Rhinella margaritifera	USNM247058, 247059, 247060, 284250; DSM0041, 0042, 0089, 0090, 0091, 0093, 0095
Rhinella poeppigii	USNM222138, 247026, 268821
Rhinella proboscidea	DSM0098, 0108
Scaphiophryne marmorata	MCZ.A-120109
Scaphiopus holbrookii	USNM529893, 529901, 529903, 529910, 529913
Scinax crospedospilus	USNM209006, 209016, 243622, 243628, 243637
Scinax garbei	USNM247216, 268906, 346331, 537709, 537710
Scinax hayii	USNM209023, 209025, 209028, 209032, 209046
Scinax ictericus	USNM222198, 222201, 247205, 247242, 247243
Scinax ruber	DSM0068−0070, 0073, 0075, 0076
Sclerophrys kisoloensis	CAS176985, 176994, 176995, 176996, 176999
Sphaenorhynchus lacteus	USNM247280, 247281, 268928, 268929, 268931; DSM0047
Staurois guttatus (as *S. natator*)	FMNH136034, 136038, 136045, 136053, 136075
Thoropa taophora	USNM209326, 209334, 209338, 209341, 209349
Tomopterna cryptotis	CAS165505, 165508, 165509, 175447, 175449
Trachycephalus venulosus	USNM247254, 247255, 247616, 343219
Uperodon triangularis	FMNH218086, 218087
Uperoleia lithomoda	DSM0257−0259
Vitreorana eurygnatha	USNM208717, 208720, 208724, 208725, 208726
Xenopus wittei	CAS201673, 201674, 201675, 201676, 201679

Note: Museum abbreviations are as follows: CAS = California Academy of Sciences; CM = Carnegie Museum; DSM = Daniel S. Moen field series; FMNH = The Field Museum; KIZ = Kunming Institute of Zoology; KU = University of Kansas Museum of Natural History; MCZ = Harvard Museum of Comparative Zoology; USNM = National Museum of Natural History, Smithsonian Institution. In some cases, museum records at the time of measurement did not match the species that was most likely what I measured (based on distribution records and recent taxonomic changes). In such cases, I list the museum's name of the specimens in parentheses.